

Quantum Optics: From Basics to Advanced topics

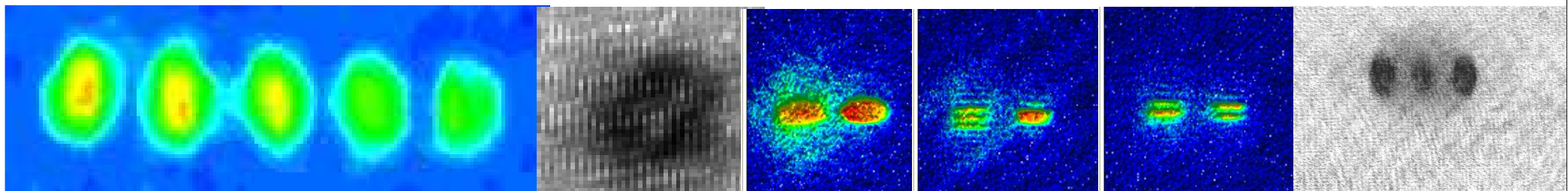
量子光学:基礎編及び展開編

Department of physics, Gakushuin University

学習院大学理学部物理学科

Takuya Hirano

平野 琢也



Self-introduction



1987年3月 東京大学理学部物理学科卒業 前半:塚田研究室, 後半:清水忠雄研究室

1987年4月～1992年3月 東京大学物性研究所松岡研究室

M1:超短パルス, CuCl中ポラリトン, M2-D3:パルス光スクイージング(町田さん)

1992年4月～1993年2月 日本学術振興会 特別研究員(PD)

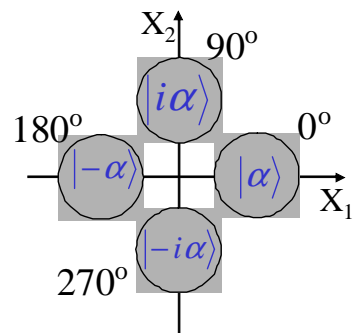
アンチバンチング(小芦さん) 連続量と離散量

1993年～1998年 東京大学久我研究室 助手

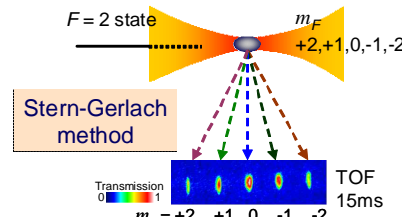
LEDによるサブポアソン光の発生, レーザー冷却(重点領域でBEC, 鳥井さん)

1998年～現在 學習院大学

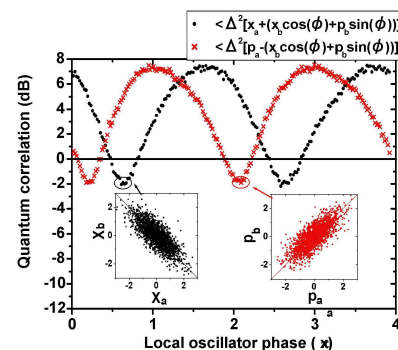
連続量の量子暗号, Rb原子BEC, パルス光スクイージング



連續量量子鍵配送



多成分凝縮体
磁力計



ループホールフリー
EPR実験、量子通信



Outline of the talk

- Introduction
- Quantization of the electromagnetic fields
- Quantum theory of light

Number states (single photon sources),
Coherent states,
Squeezed states,
Homodyne detection

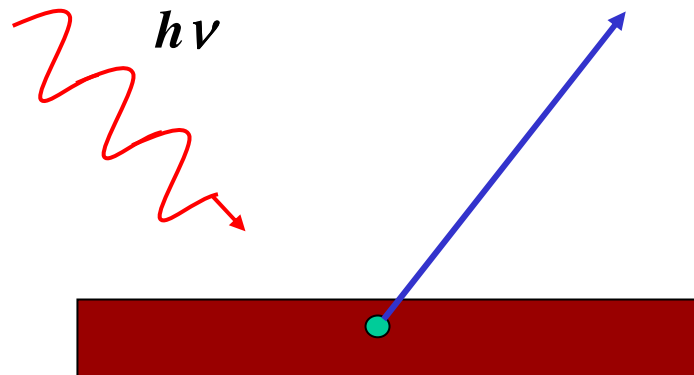
- Nonlinear optics and Quantum state control
- Correlation function
- Representation of density matrix
- Precision measurements using atoms

What is light? What is a photon ?

- ◆ Newton's particle theory
 indivisible particle, localized in space
- ◆ Electromagnetic fields described by Maxwell's equations
 vector wave
- ◆ Quantized electromagnetic theory
 wave-particle duality

In a letter to Michele Besso in 1951, Albert Einstein wrote:
“All the fifty years of conscious brooding have brought me no closer to the answer of the question: What are light quanta?
Of course, today every rascal thinks he knows the answer,
but he is deluding himself.”

Photoelectric effect



$$E_K = h\nu - \phi$$

- The ejection rate of the electrons is proportional to the intensity of the incident light.
- There exist a certain minimum frequency of the incident light below which no electrons are ejected.
- The maximum kinetic energy of the ejected electron increases as the frequency of the incident light increases, but it is independent of the intensity of the incident light.
- The time delay between the incidence of the light and the ejection of electron is very small.

“According to the concept that the incident light consists of energy quanta of magnitude $R\beta\nu/N$, however, one can conceive of the ejection of electrons by light in the following way. Energy quanta penetrate into the surface layer of the body, and their energy is transformed, at least in part, into kinetic energy of electrons. The simplest way to imagine this is that a light quantum delivers its entire energy to a single electron: we shall assume that this is what happens.”

“Concerning an Heuristic Point of View Toward the Emission and Transformation of Light,”
A. Einstein, Translation into English, American Journal of Physics, v. 33, n. 5, May 1965

Photomultiplier tubes = Photoelectric effect + Secondary emission

<http://jp.hamamatsu.com/>

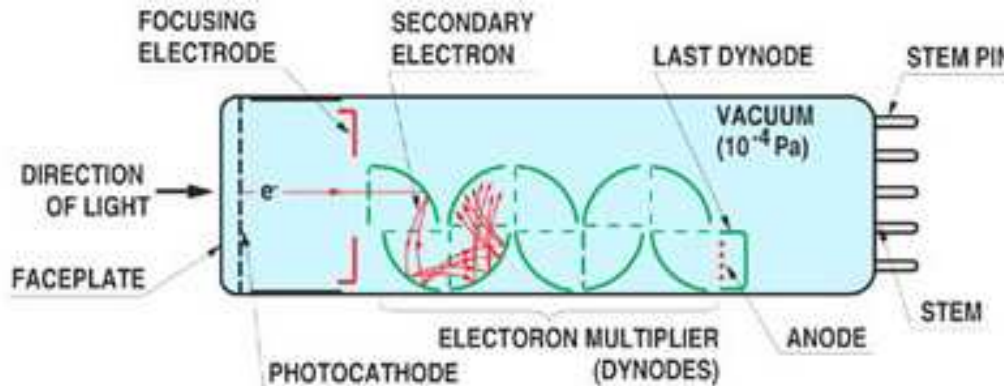


Figure 25: Overlapping Output Pulses

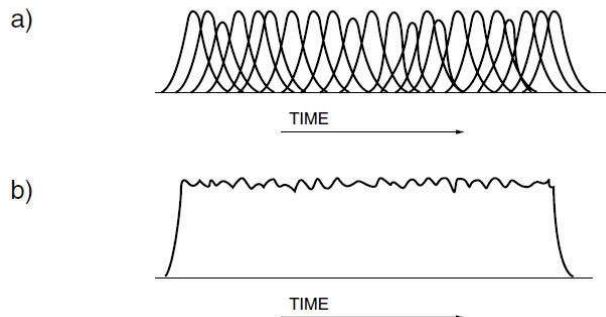


Figure 26: Discrete Output Pulses (Single Photon Event)

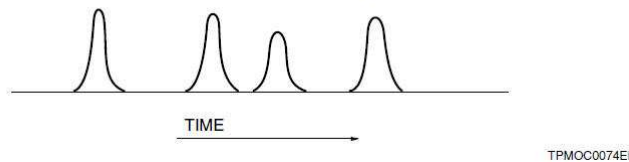
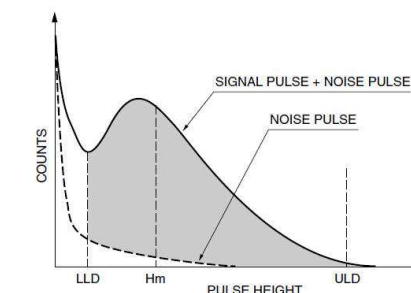
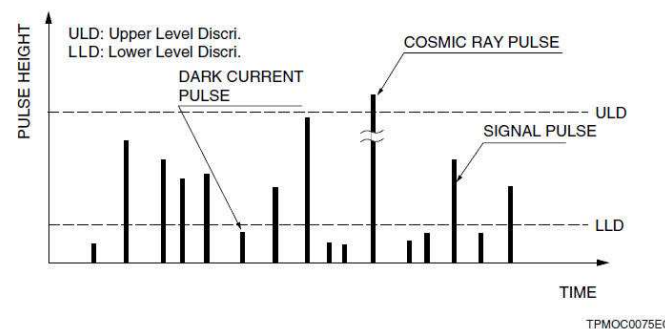
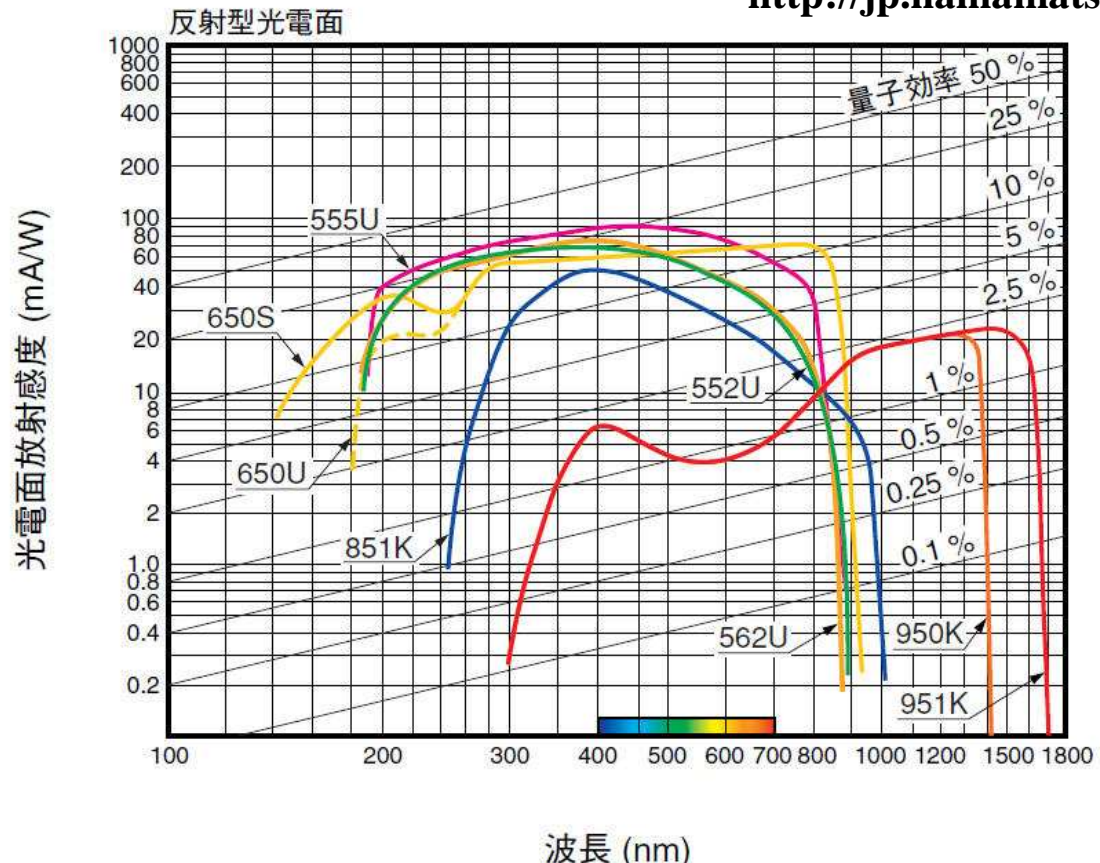


Figure 28: Typical Single Photon Pulse Height Distribution



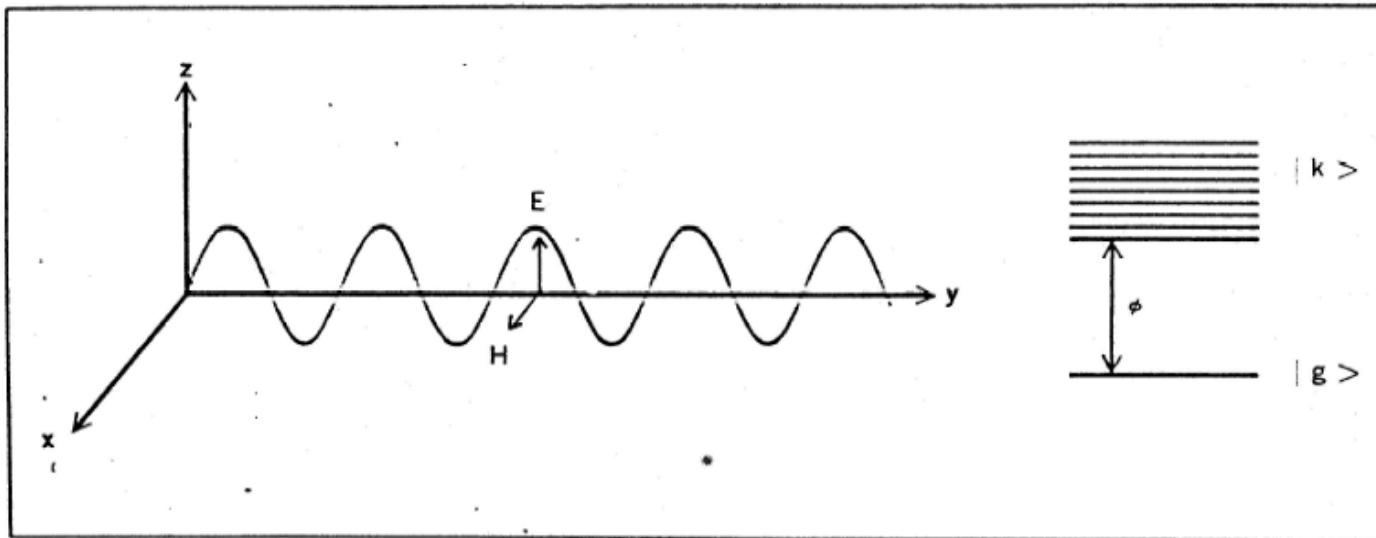
Performance of photomultiplier tubes

<http://jp.hamamatsu.com/>



Semi-classical theory of photoelectric phenomena

“The concept of the photons,” Marlan O. Scully and Murray Sargent III,
Physics Today, March 1972, p.38-47.



Photoelectric effect. An incident electromagnetic field interacts with a system in its ground state $|g\rangle$, causing transitions to occur to excited states $|k\rangle$, that is, ejecting an electron.
Figure 5.

$$\vec{E}(y, t) = \hat{z} \cos(\omega t - Ky)$$

$$H_1 = -e\vec{r} \cdot \vec{E}$$

Fermi's golden rule

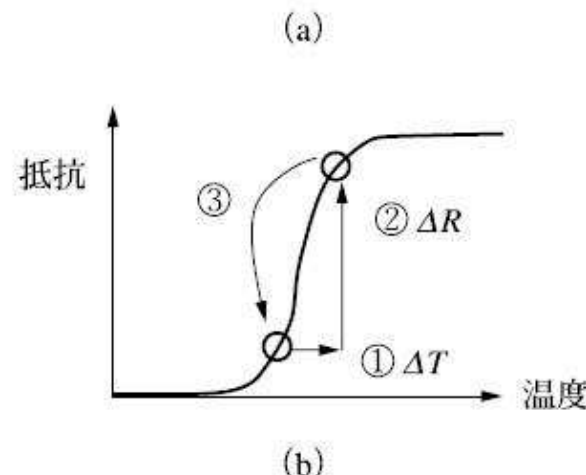
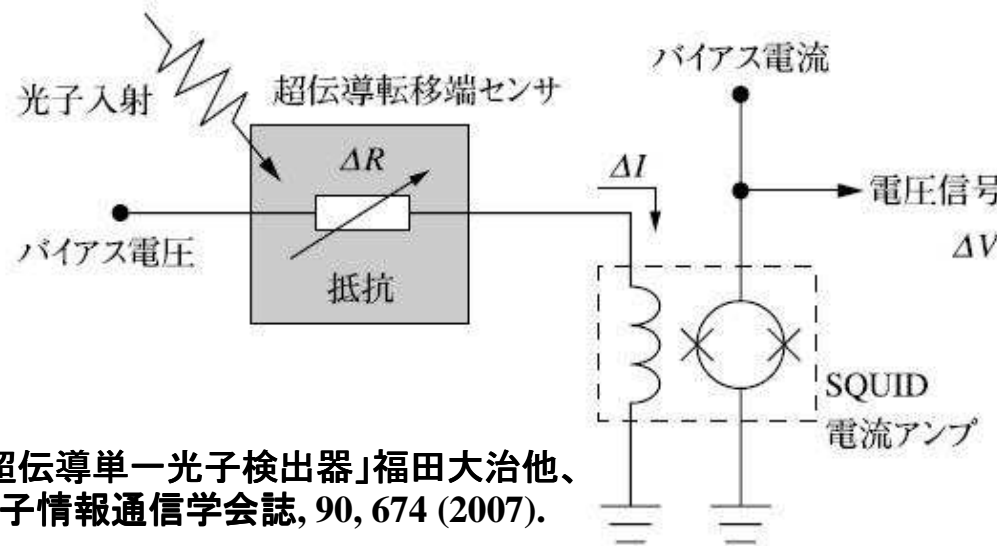
$$P_k = 2\pi [e|r_{kg}|^2 \hbar]^2 E_0^2 t \delta(\omega - (\epsilon_k - \epsilon_g)/\hbar)$$

Energy difference between the ground state and excited state

$$\epsilon_k - \epsilon_g = mv^2/2 + W$$

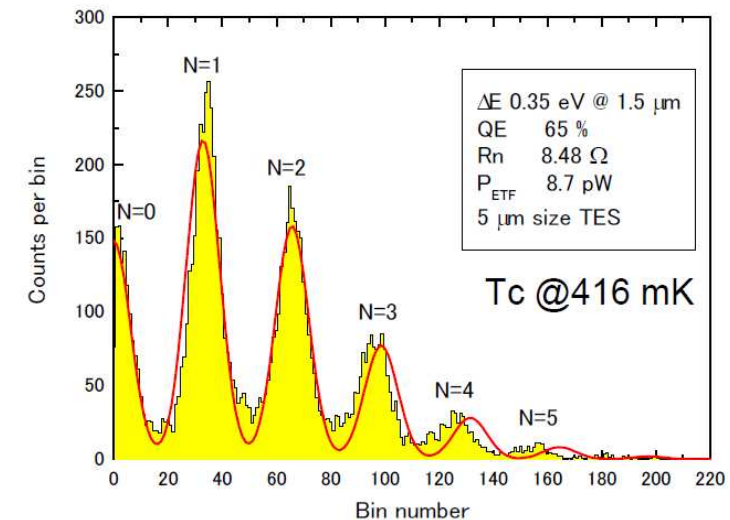
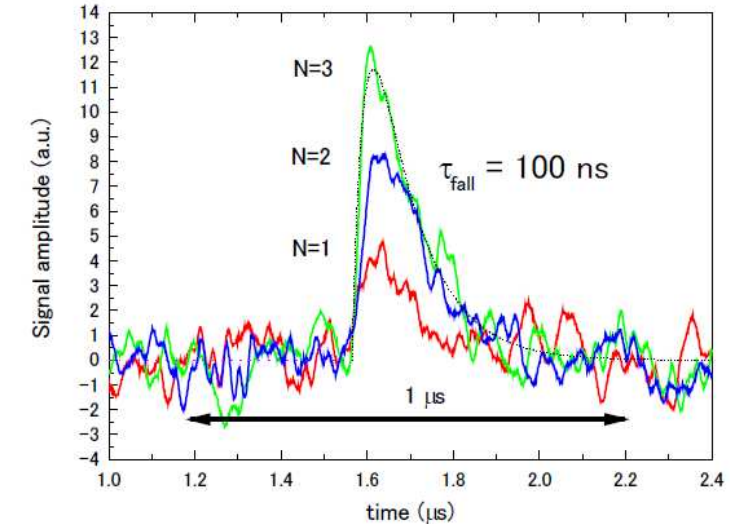
$$\rightarrow \hbar\omega = mv^2/2 + W$$

TES(Transition edge sensor): Photon number resolving detector



Opt. Express, 16, 3032, (2008): 95%@1556nm
Opt. Express, 19, 870 (2011): 98%@850nm

http://itaku-kenkyu.nict.go.jp/seika/h20/seika/90/90_aist.pdf



quantum nature of light ?

Quantum Optics: From Basics to Advanced topics

- Optical technologies continue developing drastically.
- Such development contribute both basic understanding and advanced application.
- In this talk, I would like to review the field of quantum optics emphasizing on fundamental concepts.

Outline of the talk

- Introduction
- Quantization of the electromagnetic fields

- Quantum theory of light

Number states (single photon sources),
Coherent states,
Squeezed states,
Homodyne detection

- Nonlinear optics and Quantum state control
- Correlation function
- Representation of density matrix
- Precision measurements using atoms

Quantization of the electromagnetic field

Maxwell equations

$$\left\{ \begin{array}{l} \text{rot } \vec{E} = -\frac{\partial \vec{B}}{\partial t} \\ \text{rot } \vec{B} = \mu_0 \vec{j} + \epsilon_0 \mu_0 \frac{\partial \vec{E}}{\partial t} \\ \text{div } \vec{E} = \frac{\rho}{\epsilon_0} \\ \text{div } \vec{B} = 0 \end{array} \right.$$

Potential formulation

$$\left\{ \begin{array}{l} \vec{B} = \text{rot } \vec{A} \quad (\because \text{div rot } \vec{A} = 0) \\ \vec{E} = -\text{grad } \phi - \frac{\partial \vec{A}}{\partial t} \quad (\because \text{rot grad } \phi = 0) \end{array} \right.$$

Coulomb gauge

$$\text{div } \vec{A} = 0$$

$$\left\{ \begin{array}{l} -\Delta \vec{A} + \frac{1}{c^2} \frac{\partial^2 \vec{A}}{\partial t^2} + \frac{1}{c^2} \frac{\partial}{\partial t} \text{grad } \phi = \mu_0 \vec{j} \\ -\Delta \phi = \frac{\rho}{\epsilon_0} \end{array} \right.$$

Free electromagnetic field

$$\left\{ \begin{array}{l} -\Delta \vec{A} + \frac{1}{c^2} \frac{\partial^2 \vec{A}}{\partial t^2} = 0 \quad (1-1) \\ \text{div } \vec{A} = 0 \quad (1-2) \\ \phi = 0 \end{array} \right.$$

$$\left\{ \begin{array}{l} \vec{B} = \text{rot } \vec{A} \quad (1-3) \\ \vec{E} = \frac{\partial \vec{A}}{\partial t} \quad (1-4) \end{array} \right.$$

Quantization of free electromagnetic field (1)

Plain wave expansion

$$\vec{A}(\vec{r}, t) = \sum_{\vec{k}, \sigma} \left\{ \vec{A}_{\vec{k}, \sigma}(t) \exp(i\vec{k} \cdot \vec{r}) + \vec{A}_{\vec{k}, \sigma}^*(t) \exp(-i\vec{k} \cdot \vec{r}) \right\}$$

$$\vec{k} = (k_x, k_y, k_z)$$

$$= \left(\frac{2\pi n_x}{L}, \frac{2\pi n_y}{L}, \frac{2\pi n_z}{L} \right)$$

$$n_x, n_y, n_z = 0, \pm 1, \pm 2, \dots$$

Substituting to eq. (1-2)

$$\vec{A}_{\vec{k}, \sigma}(t) \cdot \vec{k} = \vec{A}_{\vec{k}, \sigma}^*(t) \cdot \vec{k} = 0, \quad \sigma = 1, 2$$

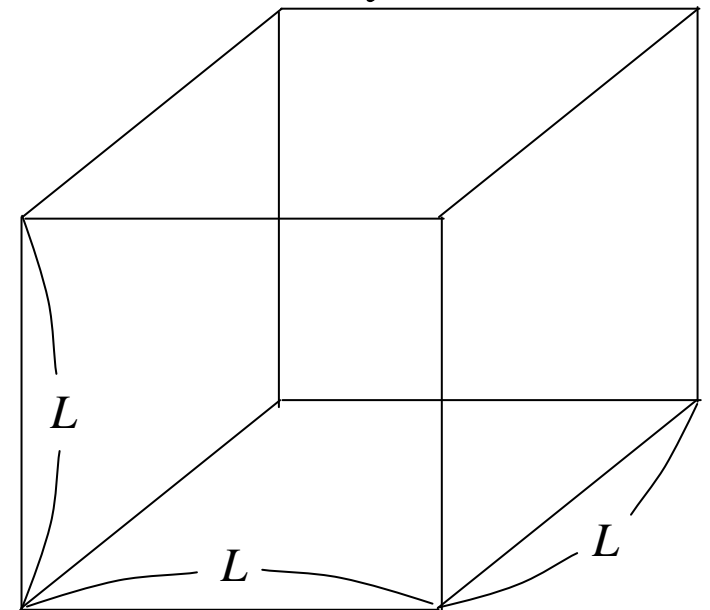
Substituting to eq. (1-1)

$$\frac{\partial^2 \vec{A}_{\vec{k}, \sigma}(t)}{\partial t^2} = -\omega_k^2 \vec{A}_{\vec{k}, \sigma}(t), \quad \omega_k = ck, \quad k = \sqrt{k_x^2 + k_y^2 + k_z^2}$$

The amplitude of each mode satisfies the same equation as a classical harmonic oscillator.

$$\vec{A}_{\vec{k}, \sigma}(t) = \vec{A}_{\vec{k}, \sigma} \exp(-i\omega_k t) \quad (1-5)$$

Periodic boundary condition



Quantization of free electromagnetic field (2)

$$\vec{A}(\vec{r}, t) = \sum_{\vec{k}, \sigma} \left\{ \vec{A}_{\vec{k}, \sigma} \exp(-i\omega_k t + i\vec{k} \cdot \vec{r}) + \vec{A}_{\vec{k}, \sigma}^* \exp(i\omega_k t - i\vec{k} \cdot \vec{r}) \right\}$$

Substituting to eq. (1-3), (1-4)

$$\vec{E}(\vec{r}, t) = \sum_{\vec{k}, \sigma} \vec{E}_{\vec{k}, \sigma}$$

$$\vec{E}_{\vec{k}, \sigma} = i\omega_k \left\{ \vec{A}_{\vec{k}, \sigma} \exp(-i\omega_k t + i\vec{k} \cdot \vec{r}) + \vec{A}_{\vec{k}, \sigma}^* \exp(i\omega_k t - i\vec{k} \cdot \vec{r}) \right\}$$

$$\vec{B}(\vec{r}, t) = \sum_{\vec{k}, \sigma} \vec{B}_{\vec{k}, \sigma}$$

$$\vec{B}_{\vec{k}, \sigma} = i\vec{k} \times \left\{ \vec{A}_{\vec{k}, \sigma} \exp(-i\omega_k t + i\vec{k} \cdot \vec{r}) + \vec{A}_{\vec{k}, \sigma}^* \exp(i\omega_k t - i\vec{k} \cdot \vec{r}) \right\}$$

Cycle-averaged energy of the electromagnetic field

$$\begin{aligned} \bar{\mathcal{E}}_{\vec{k}, \sigma} &= \frac{1}{2} \int \left(\epsilon_0 \bar{E}_{\vec{k}, \sigma}^2 + \frac{1}{\mu_0} \bar{B}_{\vec{k}, \sigma}^2 \right) dV \\ &= 2\epsilon_0 V \omega_k^2 \vec{A}_{\vec{k}, \sigma} \cdot \vec{A}_{\vec{k}, \sigma}^* \\ &= \frac{1}{2} \left(p_{\vec{k}, \sigma}^2 + \omega_k^2 q_{\vec{k}, \sigma}^2 \right) \end{aligned} \quad \left\{ \begin{array}{l} \vec{A}_{\vec{k}, \sigma} = \frac{1}{\sqrt{4\epsilon_0 V \omega_k^2}} (\omega_k q_{\vec{k}, \sigma} + i p_{\vec{k}, \sigma}) \vec{e}_{\vec{k}, \sigma} \\ \vec{A}_{\vec{k}, \sigma}^* = \frac{1}{\sqrt{4\epsilon_0 V \omega_k^2}} (\omega_k q_{\vec{k}, \sigma} - i p_{\vec{k}, \sigma}) \vec{e}_{\vec{k}, \sigma} \end{array} \right.$$

Quantization of free electromagnetic field (3)

Canonical quantization

$$[\hat{q}_{\vec{k},\sigma}, \hat{p}_{\vec{k}',\sigma'}] = i\hbar \delta_{\vec{k}\vec{k}'} \delta_{\sigma\sigma'}$$

$$\begin{aligned} \vec{A}_{\vec{k},\sigma} &= \frac{1}{\sqrt{4\epsilon_0 V \omega_k^2}} (\omega_k q_{\vec{k},\sigma} + i q_{\vec{k},\sigma}) \vec{e}_{\vec{k},\sigma} \\ &= \sqrt{\frac{\hbar}{2\epsilon_0 V \omega_k}} \hat{a}_{\vec{k},\sigma} \vec{e}_{\vec{k},\sigma} \end{aligned}$$

Anihilation and creation operators

$$\begin{cases} \hat{a}_{\vec{k},\sigma}(t) = \frac{1}{\sqrt{2\hbar\omega_k}} \{ \omega_k \hat{q}_{\vec{k},\sigma}(t) + i \hat{p}_{\vec{k},\sigma}(t) \} \\ \hat{a}_{\vec{k},\sigma}^\dagger(t) = \frac{1}{\sqrt{2\hbar\omega_k}} \{ \omega_k \hat{q}_{\vec{k},\sigma}(t) - i \hat{p}_{\vec{k},\sigma}(t) \} \end{cases}$$

➡ $[\hat{a}_{\vec{k},\sigma}(t), \hat{a}_{\vec{k}',\sigma'}^\dagger(t)] = \delta_{\vec{k}\vec{k}'} \delta_{\sigma\sigma'}$

$$\vec{A}(\vec{r}, t) = \sum_{\vec{k},\sigma} \sqrt{\frac{\hbar}{2\epsilon_0 V \omega_k}} \vec{e}_{\vec{k},\sigma} \left\{ \hat{a}_{\vec{k},\sigma} \exp(-i\omega_k t + i\vec{k} \cdot \vec{r}) + \hat{a}_{\vec{k},\sigma}^\dagger \exp(i\omega_k t - i\vec{k} \cdot \vec{r}) \right\}$$

$$\vec{E}(\vec{r}, t) = \sum_{\vec{k},\sigma} i \sqrt{\frac{\hbar\omega_k}{2\epsilon_0 V}} \vec{e}_{\vec{k},\sigma} \left\{ \hat{a}_{\vec{k},\sigma} \exp(-i\omega_k t + i\vec{k} \cdot \vec{r}) - \hat{a}_{\vec{k},\sigma}^\dagger \exp(i\omega_k t - i\vec{k} \cdot \vec{r}) \right\}$$

$$\vec{B}(\vec{r}, t) = \sum_{\vec{k},\sigma} i \sqrt{\frac{\hbar}{2\epsilon_0 V \omega_k}} \vec{k} \times \vec{e}_{\vec{k},\sigma} \left\{ \hat{a}_{\vec{k},\sigma} \exp(-i\omega_k t + i\vec{k} \cdot \vec{r}) - \hat{a}_{\vec{k},\sigma}^\dagger \exp(i\omega_k t - i\vec{k} \cdot \vec{r}) \right\}$$

Outline of the talk

- Introduction
- Quantization of the electromagnetic fields
- Quantum theory of light

Number states (single photon sources),
Coherent states,
Squeezed states,
Homodyne detection

- Nonlinear optics and Quantum state control
- Correlation function
- Representation of density matrix
- Precision measurements using atoms

Quantum states of light (1)

Hamiltonian and electric field for a single mode

$$\hat{H} = \hbar\omega \left(\hat{a}^\dagger \hat{a} + \frac{1}{2} \right)$$

$$\hat{E}(\vec{r}, t) = i \sqrt{\frac{\hbar\omega}{2\epsilon_0 V}} \left\{ \hat{a} e^{-i\omega t + i\vec{k} \cdot \vec{r}} - \hat{a}^\dagger e^{i\omega t - i\vec{k} \cdot \vec{r}} \right\}$$

Fock or number states

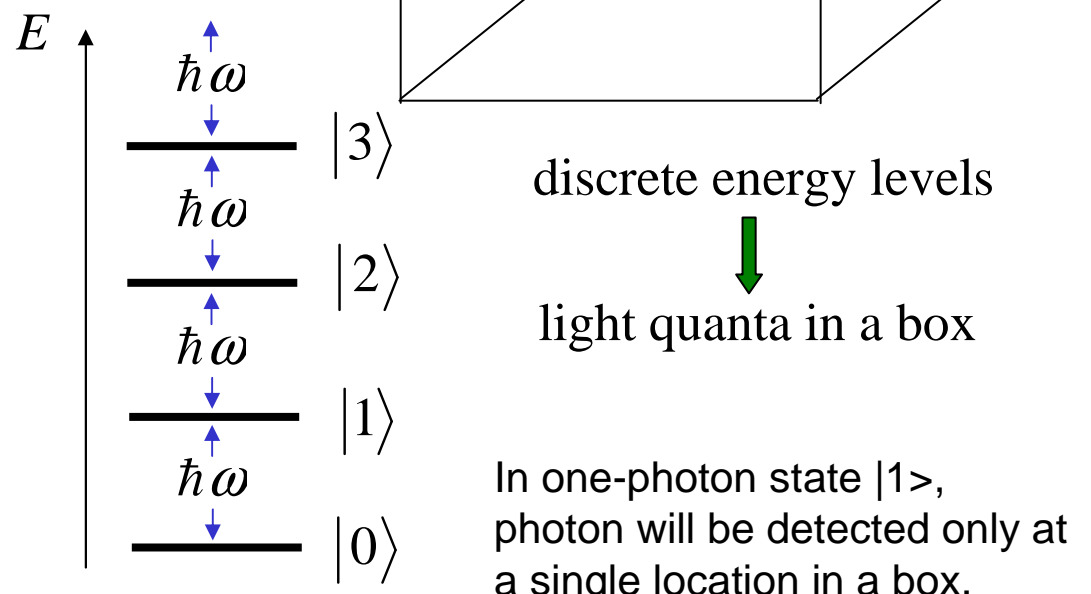
$$\hat{n}|n\rangle = n|n\rangle, \quad \hat{n} = \hat{a}^\dagger(t)\hat{a}(t)$$

$$\hat{H}|n\rangle = \hbar\omega \left(n + \frac{1}{2} \right) |n\rangle$$

$$\hat{a}|n\rangle = \sqrt{n}|n-1\rangle$$

$$\hat{a}^\dagger |n\rangle = \sqrt{n+1}|n+1\rangle$$

$|0\rangle$ ground state (vacuum state)



Fock states (2)

Expectation value of electric field

$$\hat{E}(\vec{r}, t) = i \sqrt{\frac{\hbar \omega}{2 \epsilon_0 V}} \left\{ \hat{a} e^{-i \omega t + i \vec{k} \cdot \vec{r}} - \hat{a}^\dagger e^{i \omega t - i \vec{k} \cdot \vec{r}} \right\}$$

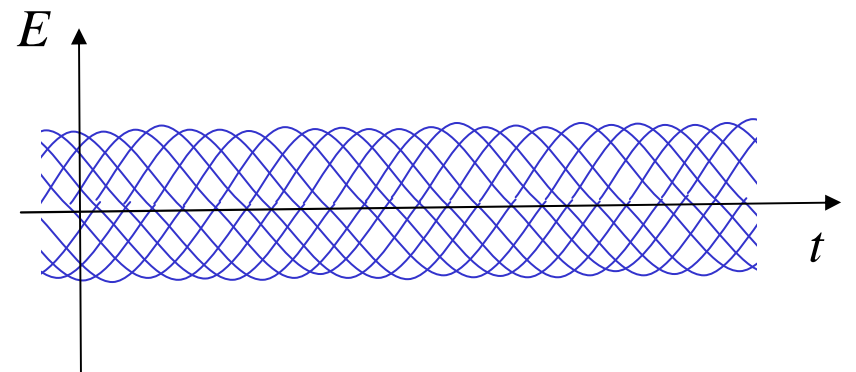
$$\langle n | \hat{E}(\vec{r}, t) | n \rangle = 0$$

$$\langle n | \hat{E}^2(\vec{r}, t) | n \rangle = \frac{\hbar \omega}{\epsilon_0 V} \left(n + \frac{1}{2} \right)$$

variance

$$(\Delta E)^2 = \left\langle (\hat{E} - \langle \hat{E} \rangle)^2 \right\rangle = \langle \hat{E}^2 \rangle - \langle \hat{E} \rangle^2$$

$$(\Delta \hat{E}) = \sqrt{\frac{\hbar \omega}{\epsilon_0 V}} \sqrt{n + \frac{1}{2}}$$



Phase is indefinite.

There exist vacuum fluctuations.
Wave ?

Fock states (3)

Description of multimode fields

$$\hat{H} = \sum_{\vec{k}, \sigma} \hat{H}_{\vec{k}, \sigma} \quad , \quad \hat{H}_{\vec{k}, \sigma} = \hbar \omega_k \left(\hat{a}_{\vec{k}, \sigma}^\dagger \hat{a}_{\vec{k}, \sigma} + \frac{1}{2} \right)$$

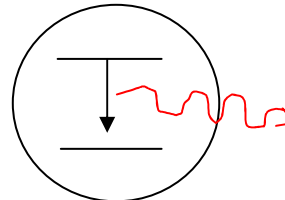
$$\hat{H}_{\vec{k}, \sigma} |n_{\vec{k}, \sigma}\rangle = \hbar \omega_k \left(n_{\vec{k}, \sigma} + \frac{1}{2} \right) |n_{\vec{k}, \sigma}\rangle$$

$$|n_{\vec{k}_1, \sigma_1}\rangle \otimes |n_{\vec{k}_1, \sigma_2}\rangle \otimes \cdots \otimes |n_{\vec{k}_j, \sigma_j}\rangle \otimes \cdots = |n_{\vec{k}_1, \sigma_1}, n_{\vec{k}_1, \sigma_2}, \dots, n_{\vec{k}_j, \sigma_j}, \dots\rangle = |\{n_{\vec{k}, \sigma}\}\rangle$$

$$\begin{aligned} |\psi\rangle &= \sum_{n_{\vec{k}_1, \sigma_1}} \sum_{n_{\vec{k}_1, \sigma_2}} \cdots \sum_{n_{\vec{k}_j, \sigma_j}} \cdots C_{n_{\vec{k}_1, \sigma_1}} C_{n_{\vec{k}_1, \sigma_2}} \cdots C_{n_{\vec{k}_j, \sigma_j}} \cdots |n_{\vec{k}_1, \sigma_1}, n_{\vec{k}_1, \sigma_2}, \dots, n_{\vec{k}_j, \sigma_j}, \dots\rangle \\ &= \sum_{\{n_{\vec{k}, \sigma}\}} C_{\{n_{\vec{k}, \sigma}\}} |\{n_{\vec{k}, \sigma}\}\rangle \end{aligned}$$

Single photons sources

Single atom



Phys. Rev. Lett.
39, 691 (1977).

Single photon sources

- Single atoms, molecules
- Single “artificial” atoms
- Quantum dots
- Nitrogen vacancies in diamond
- Correlated photons sources
- Spontaneous parametric downconversion
- For wave mixing
- Attenuated laser as “quasi” single photon

Two photon correlations will be discussed later.

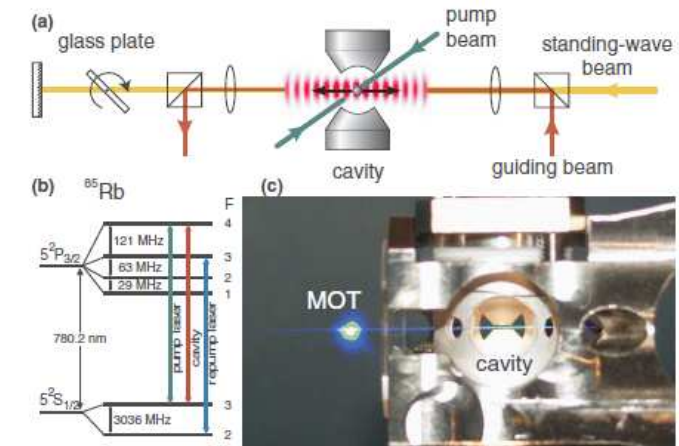


FIG. 1 (color online). Experimental setup: (a) Sketch of the dipole-trap arrangement that is used to guide atoms into the cavity. A standing-wave dipole-force trap allows us to freely adjust the position of an atom within the cavity mode by tilting a thick glass plate in front of the retro-reflecting mirror. Atoms that are trapped in the antinodes are displaced accordingly. (b) Level-scheme of ^{85}Rb including the relevant transitions. (c) Side view of the cavity (cone-shaped mirrors), superimposed with absorption images of an atom cloud in the MOT and in the transport trap illustrating the path of the atoms.

delivering up to 300,000 photons for up to 30 s.

"A single-photon server with just one atom", Markus Hijkema, et al., Nature Physics, 3, 253 (2007)

Coherent states (1)

Eigenstates of annihilation operator

$$\hat{a}|\alpha\rangle = \alpha|\alpha\rangle, \quad \alpha \text{ is a complex number.}$$

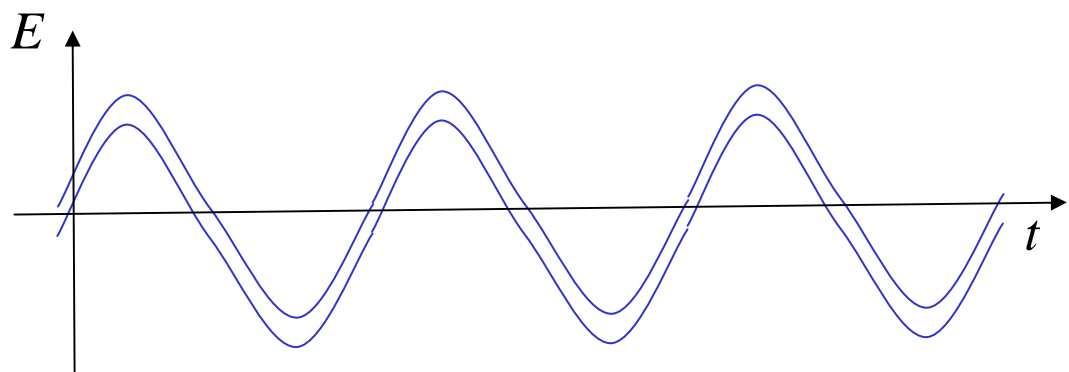
$$\begin{aligned}\bar{n} &= \langle \alpha | \hat{n} | \alpha \rangle \\ &= \langle \alpha | \hat{a}^\dagger \hat{a} | \alpha \rangle \\ &= \langle \alpha | \alpha^* \alpha | \alpha \rangle \\ &= |\alpha|^2\end{aligned}$$

$$(\Delta n)^2 = |\alpha|^2$$

$$\langle \alpha | \hat{E}(\vec{r}, t) | \alpha \rangle = 2 \sqrt{\frac{\hbar \omega_k}{2 \epsilon_0 V}} |\alpha| \sin(\omega t - \vec{k} \cdot \vec{r} - \theta), \quad \alpha = |\alpha| e^{i\theta}$$

$$\langle n | \hat{E}^2(\vec{r}, t) | n \rangle = \frac{\hbar \omega_k}{2 \epsilon_0 V} \left\{ 4 |\alpha|^2 \sin^2(\omega t - \vec{k} \cdot \vec{r} - \theta) + 1 \right\}$$

$$\Rightarrow (\Delta E)^2 = \frac{\hbar \omega_k}{2 \epsilon_0 V} \quad \text{Independent of } \alpha, r \text{ and } t$$



$$\frac{\Delta E}{\text{Amplitude}} = \frac{1}{2|\alpha|} = \frac{1}{2\sqrt{n}}$$

Negligible for ordinary lasers.

Coherent states (2)

Expansion of $|\alpha\rangle$ in terms of $|n\rangle$

$$|\alpha\rangle = e^{-|\alpha|^2/2} \sum_{n=0}^{\infty} \frac{\alpha^n}{\sqrt{n!}} |n\rangle$$

$$\langle n|\alpha\rangle^2 = e^{-|\alpha|^2} \frac{|\alpha|^n}{n!} \quad \text{Poissonian distribution}$$

$$\langle\alpha|\beta\rangle^2 = e^{-|\alpha-\beta|^2} \quad \text{Coherent states are nonorthogonal.}$$

Displacement operator

$$\begin{aligned} \hat{D}(\alpha) &= e^{\alpha\hat{a}^\dagger - \alpha^*\hat{a}} \\ &= e^{-|\alpha|^2/2} e^{\alpha\hat{a}^\dagger} e^{-\alpha^*\hat{a}} \\ (\because e^{\hat{A}+\hat{B}+[\hat{A},\hat{B}]} &= e^{\hat{A}}e^{\hat{B}} \\ \text{if } [\hat{A},[\hat{A},\hat{B}]] &= [\hat{B},[\hat{A},\hat{B}]] = 0) \end{aligned}$$

$$|\alpha\rangle = \hat{D}(\alpha)|0\rangle$$

Three definitions are equivalent except for a phase.

- $\hat{a}|\alpha\rangle = \alpha|\alpha\rangle$
- $|\alpha\rangle = e^{-|\alpha|^2/2} \sum_{n=0}^{\infty} \frac{\alpha^n}{\sqrt{n!}} |n\rangle$
- $|\alpha\rangle = \hat{D}(\alpha)|0\rangle, \quad \hat{D}(\alpha) = e^{\alpha\hat{a}^\dagger - \alpha^*\hat{a}}$

$$\begin{cases} \hat{D}^\dagger(\alpha)\hat{a}\hat{D}(\alpha) = \hat{a} + \alpha \\ \hat{D}^\dagger(\alpha)\hat{a}^\dagger\hat{D}(\alpha) = \hat{a}^\dagger + \alpha^* \end{cases}$$

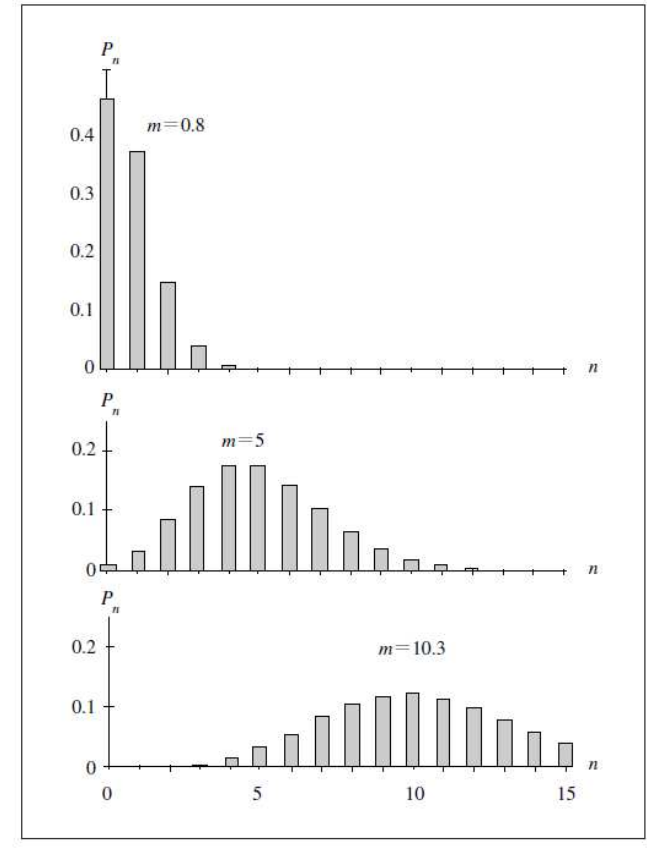


図1 ポアソン分布 「基礎からの量子光学」松岡正浩

Coherent states (3)

Quadrature phase amplitude

$$\begin{cases} \hat{x}_1 = \frac{1}{2}(\hat{a} + \hat{a}^\dagger) \\ \hat{x}_2 = \frac{1}{2}(-i\hat{a} + i\hat{a}^\dagger) \end{cases}$$

$$[\hat{x}_1, \hat{x}_2] = \frac{i}{2}$$

$$(\Delta \hat{x}_1)(\Delta \hat{x}_2) \geq \frac{1}{4}$$

$$\begin{aligned} \hat{E}(\vec{r}, t) &= i \sqrt{\frac{\hbar \omega}{2 \varepsilon_0 V}} \left\{ \hat{a} e^{-i\omega t + i\vec{k} \cdot \vec{r}} - \hat{a}^\dagger e^{i\omega t - i\vec{k} \cdot \vec{r}} \right\} \\ &= \sqrt{\frac{2\hbar\omega}{\varepsilon_0 V}} \left\{ \hat{x}_1 \cos(\omega t - \vec{k} \cdot \vec{r} - \frac{\pi}{2}) \right. \\ &\quad \left. + x_2 \sin(\omega t - \vec{k} \cdot \vec{r} - \frac{\pi}{2}) \right\} \end{aligned}$$

$$\langle \alpha | \hat{x}_1 | \alpha \rangle = \frac{\alpha + \alpha^*}{2}$$

$$\langle \alpha | \hat{x}_1^2 | \alpha \rangle = \left(\frac{\alpha + \alpha^*}{2} \right)^2 + \frac{1}{4}$$

$$(\langle \alpha | \hat{x}_1^2 | \alpha \rangle = \langle \alpha | \frac{\hat{a}^2 + \hat{a}\hat{a}^\dagger + \hat{a}^\dagger\hat{a} + \hat{a}^{\dagger 2}}{4} | \alpha \rangle = \langle \alpha | \frac{\hat{a}^2 + \hat{a}^\dagger\hat{a} + 1 + \hat{a}^\dagger\hat{a} + \hat{a}^{\dagger 2}}{4} | \alpha \rangle)$$

$$\rightarrow (\Delta x_1)^2 = \frac{1}{4}$$

$$(\Delta x_1) = (\Delta x_2) = \frac{1}{2}$$

$$\rightarrow (\Delta x_1)(\Delta x_2) = \frac{1}{4}$$

Coherent state is a minimum uncertainty state with equal variance.

Squeezed states (1)

Squeeze operator

$$\hat{S}(\zeta) = \exp\left\{\frac{1}{2}\left(\zeta^*\hat{a}^2 - \zeta\hat{a}^{\dagger 2}\right)\right\}, \quad \zeta = re^{i\varphi}$$

$$\begin{cases} \hat{S}^\dagger(\zeta)\hat{a}\hat{S}(\zeta) = \hat{a}\cosh r - \hat{a}^\dagger e^{i\varphi} \sinh r \\ \hat{S}^\dagger(\zeta)\hat{a}^\dagger\hat{S}(\zeta) = \hat{a}^\dagger\cosh r - \hat{a}e^{-i\varphi} \sinh r \end{cases}$$

$$(\because e^{\hat{A}}\hat{B}e^{-\hat{A}} = \hat{B} + [\hat{A}, \hat{B}] + \frac{1}{2!}[\hat{A}, [\hat{A}, \hat{B}]] + \dots)$$

Squeezed states may be defined as,

$$|\zeta, \alpha\rangle \equiv \hat{S}(\zeta)|\alpha\rangle = \hat{S}(\zeta)\hat{D}(\alpha)|0\rangle$$

then,

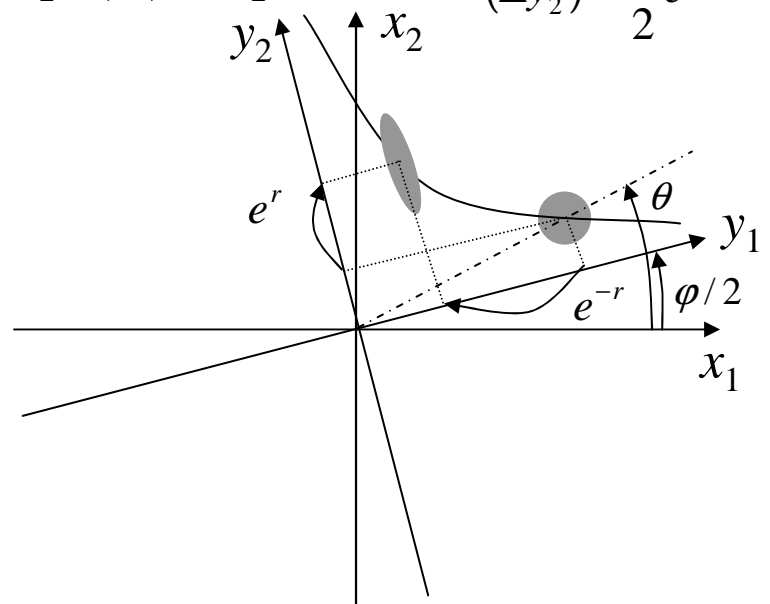
$$\langle \zeta, \alpha | \hat{a} | \zeta, \alpha \rangle = \alpha \cosh r - \alpha^* e^{i\varphi} \sinh r$$

Quadrature phase amplitude

$$\begin{aligned} \hat{a} &= \hat{x}_1 + i\hat{x}_2 \\ &= e^{i\varphi/2}(\hat{y}_1 + i\hat{y}_2) \end{aligned} \quad \begin{pmatrix} \hat{x}_1 \\ \hat{x}_2 \end{pmatrix} = \begin{pmatrix} \cos\varphi/2 & -\sin\varphi/2 \\ \sin\varphi/2 & \cos\varphi/2 \end{pmatrix} \begin{pmatrix} \hat{y}_1 \\ \hat{y}_2 \end{pmatrix}$$

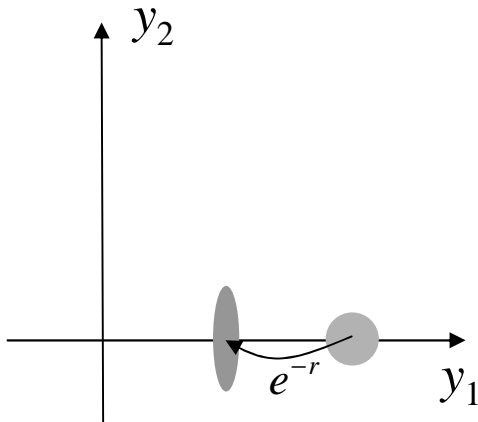
$$\langle \hat{a} \rangle = e^{i\varphi/2}(\langle \hat{y}_1 \rangle + i\langle \hat{y}_2 \rangle)$$

$$\begin{cases} \hat{S}^\dagger(\zeta)\hat{y}_1\hat{S}(\zeta) = \hat{y}_1 e^{-r} \\ \hat{S}^\dagger(\zeta)\hat{y}_2\hat{S}(\zeta) = \hat{y}_2 e^r \end{cases} \quad \begin{cases} (\Delta y_1) = \frac{1}{2}e^{-r} \\ (\Delta y_2) = \frac{1}{2}e^r \end{cases}$$



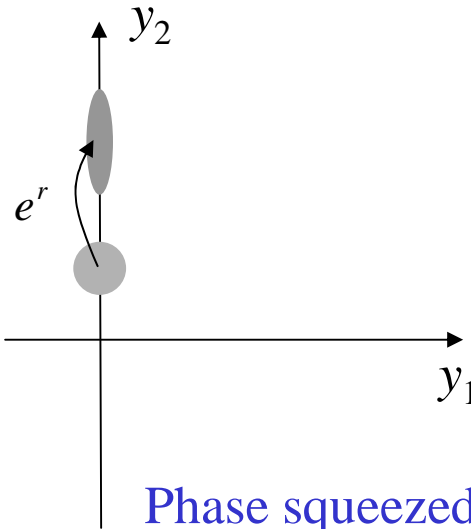
Squeezed states (2)

If $\theta = \varphi = 0$,

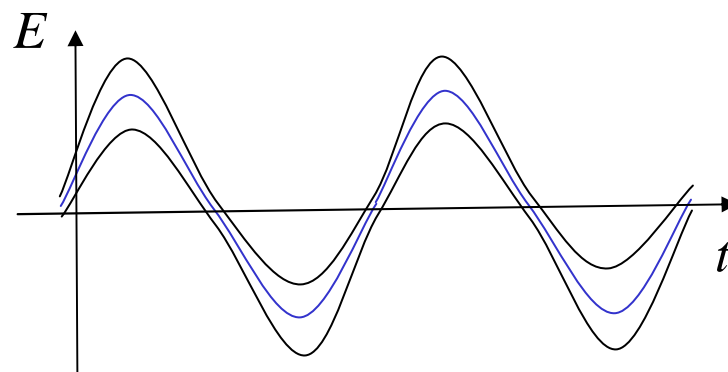
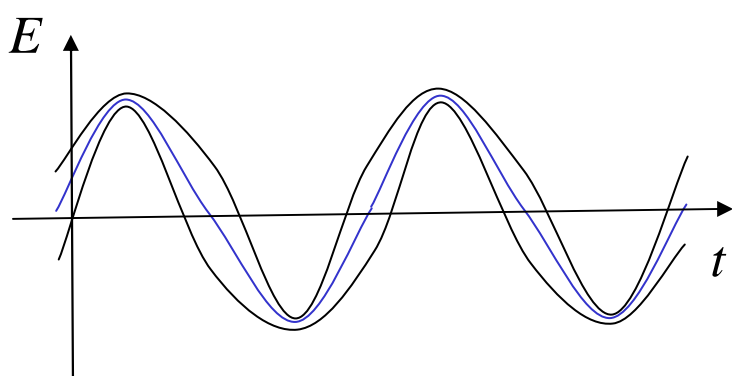


Amplitude squeezed state

If $\theta = \pi/2, \varphi = 0$,



Phase squeezed state



Figures are inaccurate, sorry.

Squeezed states (3)

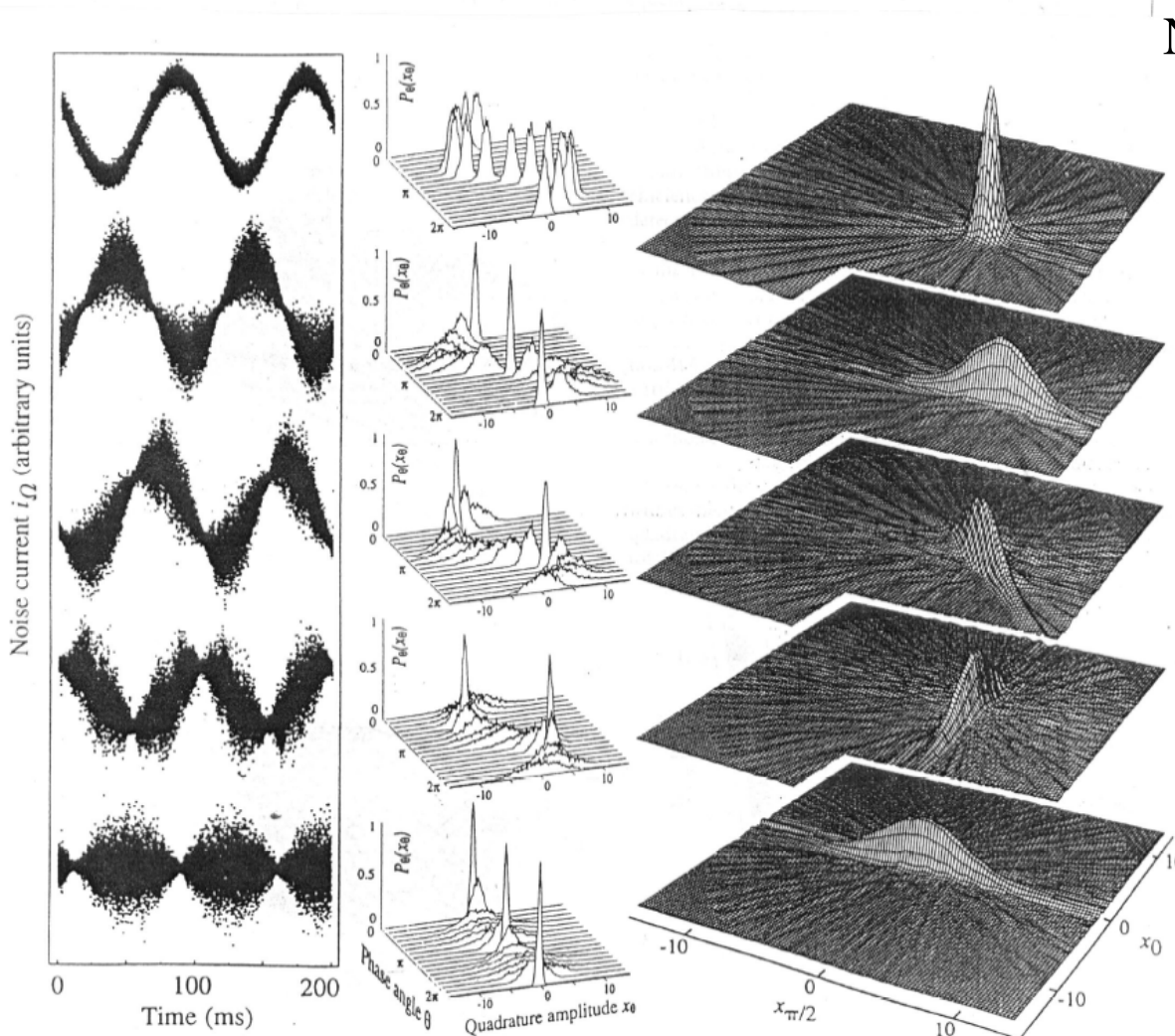


Figure 2 Noise traces in $i_B(t)$ (left), quadrature distributions $P_{\theta}(x_0)$ (centre), and reconstructed Wigner functions (right) of generated quantum states. From the top: Coherent state, phase-squeezed state, state squeezed in the $\phi = 48^\circ$ -quadrature, amplitude-squeezed state, squeezed vacuum state. The noise traces as a function of time show the electric fields' oscillation in a 4π interval for the upper

four states, whereas for the squeezed vacuum (belonging to a different set of measurements) a 3π interval is shown. The quadrature distributions (centre) can be interpreted as the time evolution of wave packets (position probability densities) during one oscillation period. For the reconstruction of the quantum states a π interval suffices.

Nature 387, 472 (1997)

Quadrature amplitudes were measured by homodyne detection.

Quantum states of a single-mode EM field

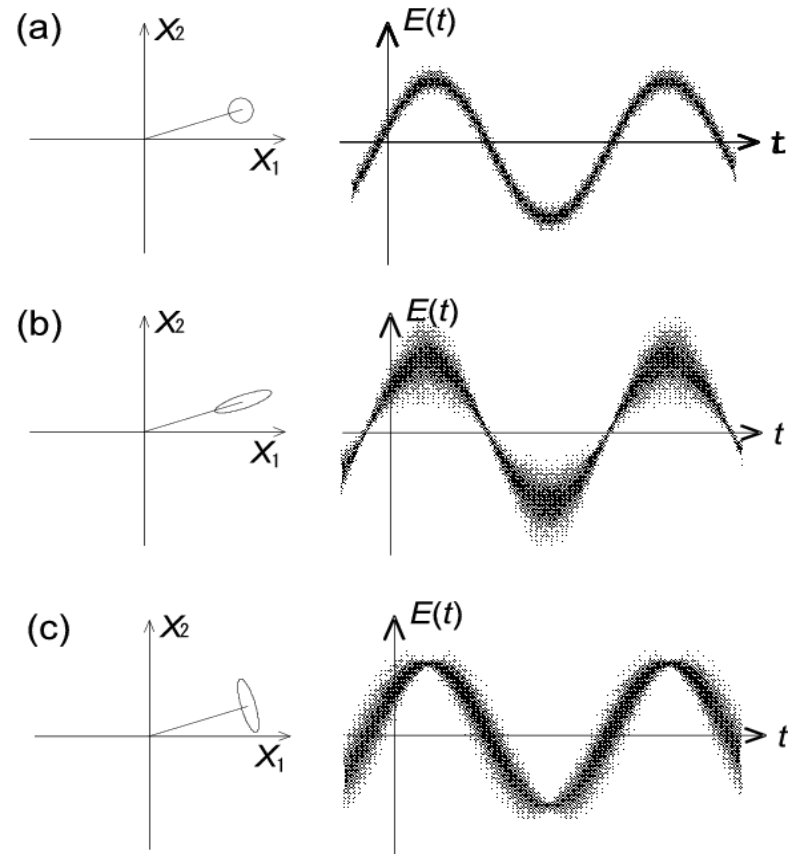
Fock states $|n\rangle = \frac{1}{\sqrt{n!}} (\hat{a}^\dagger)^n |0\rangle$

Coherent states $|\alpha\rangle = \hat{D}(\alpha)|0\rangle$,

$$\hat{D}(\alpha) = \exp(\alpha \hat{a}^\dagger - \alpha^* \hat{a})$$

Squeezed states $|\zeta, \alpha\rangle = \hat{S}(\zeta)|\alpha\rangle$,

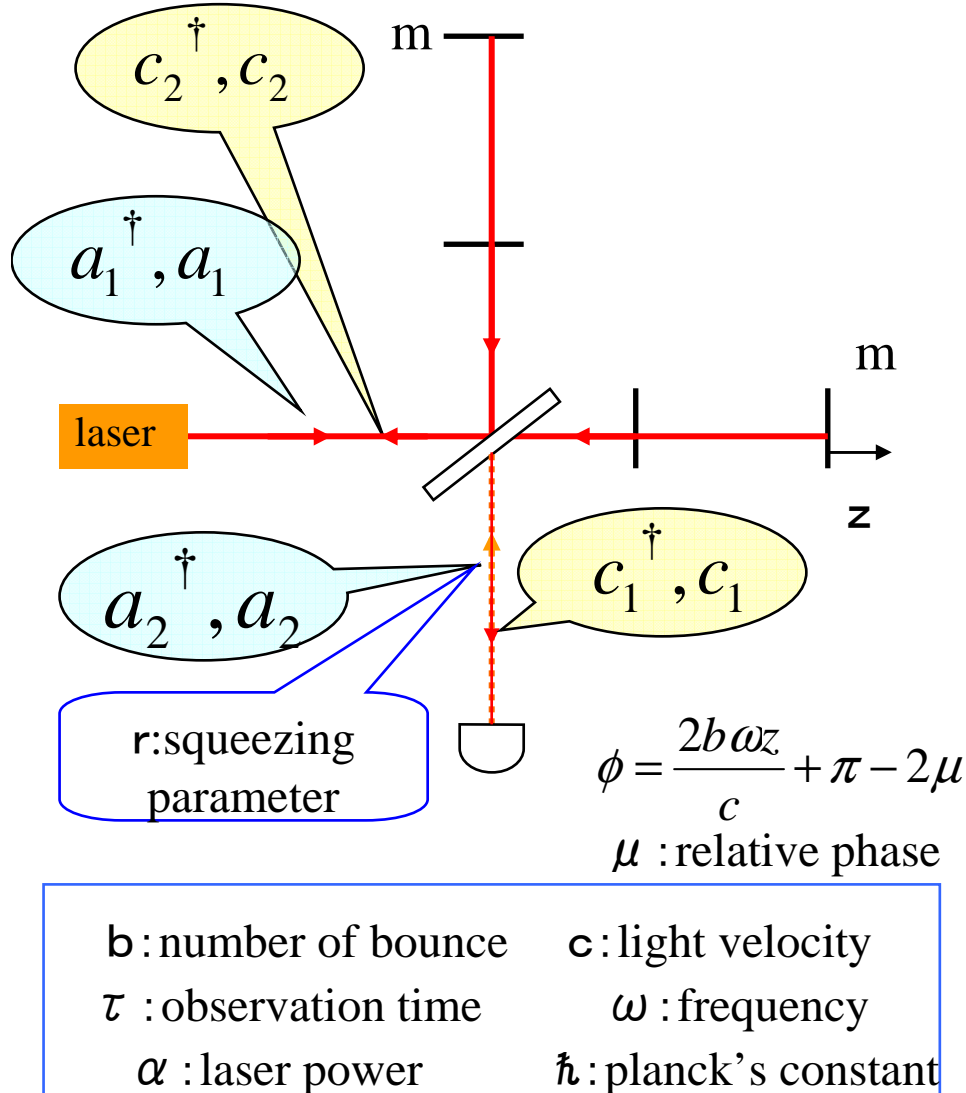
$$\hat{S}(\zeta) = \exp(\zeta^* \hat{a}^2 - \alpha \hat{a}^{\dagger 2})/2$$



However, in experiments, a quantum state of a plane-wave mode are not observed in most cases.

Quantum-enhanced gravitational-wave detector

"Quantum-mechanical noise in an interferometer," Carlton M. Caves, Phys. Rev. D, 23, 1693 (1981).



Photon counting error

$$n_{out} \equiv c_1^\dagger c_1 \quad z \rightarrow z + \delta z$$

$$\delta n_{out} \equiv \alpha^2 \left(\frac{2b\omega}{c} \right) \sin\left(\frac{\phi}{2}\right) \cos\left(\frac{\phi}{2}\right) \delta z \quad \frac{\Delta z}{\delta z} = \frac{\Delta n_{out}}{\delta n_{out}}$$

$$(\Delta z)_{pc} \equiv \left(\frac{c}{2b\omega} \right) \left(\frac{e^{-2r}}{\alpha^2} + \frac{\sinh^2 r}{\alpha^4} \right)^{\frac{1}{2}}$$

Radiation pressure error

$$\wp \equiv \left(\frac{2b\hbar\omega}{c} \right) (b_2^\dagger b_2 - b_1^\dagger b_1)$$

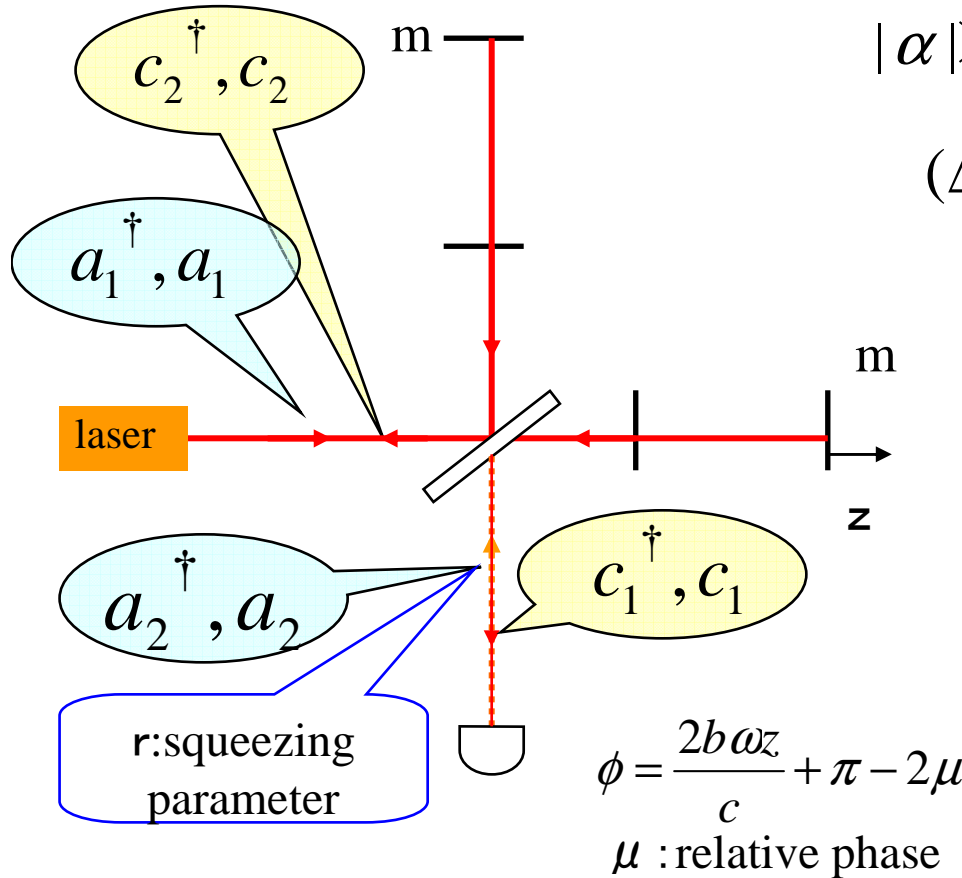
$$(\Delta \wp)^2 = \left(\frac{c}{2b\hbar\omega} \right)^2 (\alpha^2 e^{2r} + \sinh^2 r)$$

$$(\Delta z)_{rp} \equiv \frac{(\Delta \wp)\tau}{2m}$$

$$= \left(\frac{b\hbar\omega\tau}{mc} \right) \left(\alpha^2 e^{2r} + \sinh^2 r \right)^{\frac{1}{2}}$$

Quantum-enhanced gravitational-wave detector

"Quantum-mechanical noise in an interferometer," Carlton M. Caves, Phys. Rev. D, 23, 1693 (1981).



b : number of bounce

τ : observation time

α : laser power

c : light velocity

ω : frequency

\hbar : planck's constant

$$|\alpha| \gg \sinh^2 r$$

$$(\Delta z)_{rp} \sim \left(\frac{b\hbar\omega\tau}{mc} \right) |\alpha| e^r \quad (\Delta z)_{pc} \sim \left(\frac{c}{2b\omega} \right) \frac{e^{-r}}{|\alpha|}$$

$$\Delta z = \{ (\Delta z)_{pc}^2 + (\Delta z)_{rp}^2 \}^{1/2}$$

Minimum when $(\Delta z)_{pc} = (\Delta z)_{rp}$

$$|\alpha|^2 = \frac{1}{2} \left(\frac{mc^2}{\hbar\omega} \right) \left(\frac{1}{\omega\tau} \right) \left(\frac{1}{b^2} \right) e^{-2r} = \alpha_{opt}^2$$

$$\Delta z_{opt} = \left(\frac{\hbar\tau}{m} \right)^{1/2} \cong (\Delta z)_{SQL}$$

A Quantum-enhanced prototype gravitational-wave detector

K. Goda, et al. Nature Physics, 4, 472 (2008).

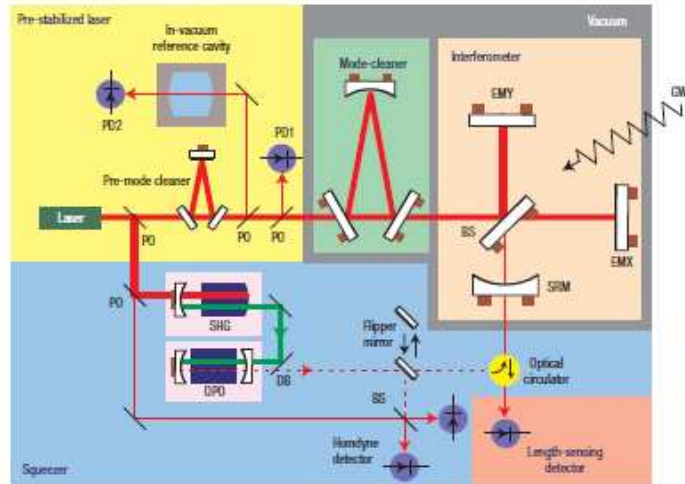


Figure 1 Schematic diagram of the quantum-enhanced prototype gravitational-wave detector that consists of five parts. BS: 50/50 beamsplitter; PD1 and PD2: photodetectors; PO: pickoff beamsplitter; DB: dichroic beamsplitter; SRM: signal-recycling mirror; EMX/EMY: end mirrors along the x/y axis, respectively; SHG: second-harmonic generator; OPO: optical parametric oscillator; GW: gravitational wave. The SHG, OPO, reference cavity, pre-mode cleaner, mode-cleaner and signal-recycling cavity are all locked by adaptations of Pound-Drever-Hall locking¹⁷. PD1 and PD2 are used for the laser intensity and frequency stabilization, whereas two photodetectors in the interferometer (not shown) and the length-sensing detector are used to control the interferometer. All of the mode-cleaner and interferometer optics are suspended by single-loop pendulums.

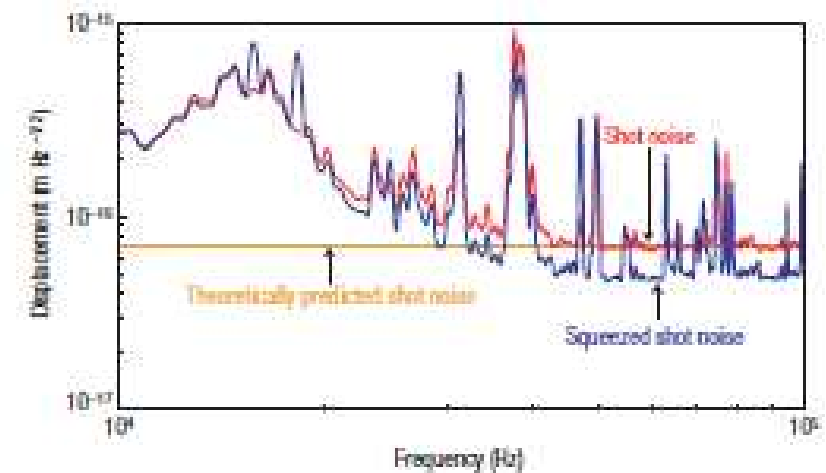


Figure 2 The noise floor of the signal-recycled Michelson interferometer with (blue) and without (red) the injection of squeezed vacuum. The theoretically predicted shot-noise level based on the measured optical power is also shown (orange). The interferometer is shot-noise-limited at frequencies above 42 kHz. Injection of squeezing leads to broadband reduction of the shot noise in the shot-noise-limited frequency band.

44% improvement in displacement sensitivity of a prototype gravitational-wave detector with suspended quasi-free mirrors

Pulsed light as a single mode

“Optical coherence and quantum optics”, L. Mandel and E. Wolf, p.480 and 12.11.5.
We have defined photons as quantum excitations of the normal modes of the electromagnetic field, and we have associated them with plane waves of definite wave vector and definite polarization.

Now a plane wave has no localization in space or time, and therefore the excitation in the one-photon state $\hat{a}_\lambda^\dagger |0\rangle$ must be regarded as distributed over all space-time.

We may define a one-photon state localized in space by a linear superposition,

$$|\phi\rangle = \sum_{\lambda} \phi(\lambda) \hat{a}_\lambda^\dagger |0\rangle, \quad \langle \phi | \phi \rangle = \sum_{\lambda} |\phi(\lambda)|^2 = 1,$$

the corresponding spatial-temporal wave function is

$$\vec{\Phi}(\vec{r}, t) = \sum_{\lambda} \phi(\lambda) \vec{u}_{\lambda}(\vec{r}) \exp(-i\omega_{\lambda} t) \quad (\text{IP}).$$

$|\phi\rangle$ is an eigenstate of the total photon number operator \hat{n}

$$\hat{n}|\phi\rangle = 1 \cdot |\phi\rangle, \quad \hat{n} = \sum_{\lambda} \hat{n}_{\lambda} = \sum_{\lambda} \hat{a}_\lambda^\dagger \hat{a}_\lambda$$

If we define a new operator $\hat{c} = \sum_{\lambda} \phi^*(\lambda) \hat{a}_\lambda$,

$$|\phi\rangle = \hat{c}^\dagger |0\rangle, \quad [\hat{c}^\dagger, \hat{c}] = 1$$

Any spatial-temporal mode can be regarded as a single mode.

Generation of squeezed states

Moritz Mehmet *et al.* Phys. Rev. A81, 013814 (2010).

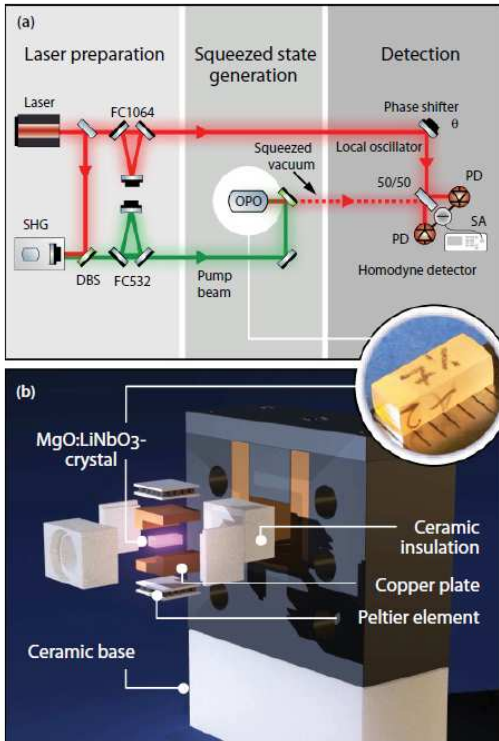


FIG. 1. (Color) Experimental apparatus. (a) Schematic diagram of the experimental setup. A small part of the 1064-nm output of the 2-W laser system was used as local oscillator while the majority was sent to an external second-harmonic generation (SHG) cavity which provided the 532-nm pump beam to drive the OPO. Travelling wave filter cavities (FC1064 and FC532) in both paths were used to provide stable and well-defined laser beams. Squeezed vacuum states at 1064 nm were generated by type I OPO below threshold in a nonlinear monolithic cavity. A balanced homodyne detector was used to measure the states' quadrature variances. DBS, dichroic beam splitter; PD, photo diode; SA, spectrum analyzer. (b) Exploded assembly drawing of the oven enclosing the squeezed light source. The nonlinear crystal, copper plates, Peltier elements, and thermal insulations are shown. The inset shows a photograph of the monolithic squeezed light source made from 7% doped MgO:LiNbO₃.

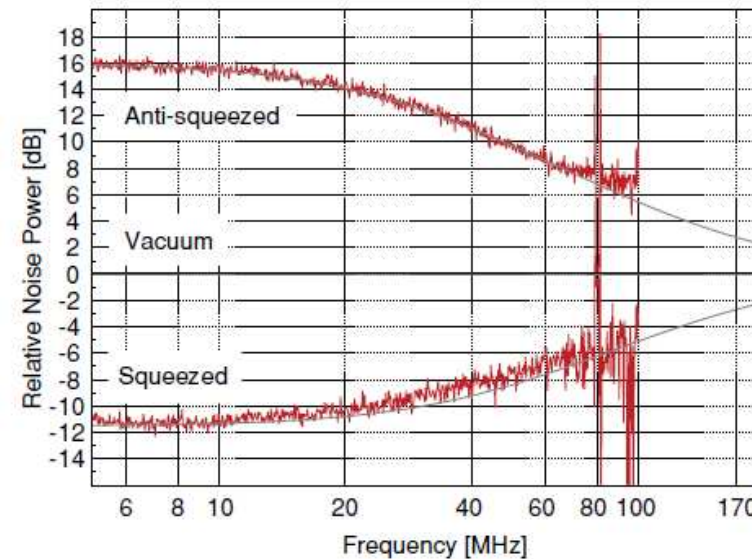


FIG. 6. (Color online) High-bandwidth squeezing spectrum. Squeezing (bottom trace) and antisqueezing (top trace) are shown relative to the vacuum noise variance. The measurements were performed from 5 to 100 MHz. This was limited by the fact that the dark noise clearance of the homodyne detector was too low toward higher frequencies. The traces are averages of three measurements each done with a resolution bandwidth of 1 MHz and a video bandwidth of 3 kHz. The data were fitted to a model and revealed a squeezing bandwidth of 170 MHz (thin line).

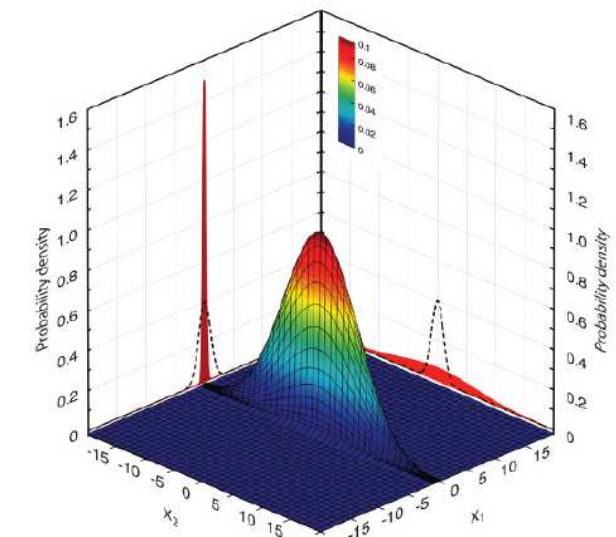
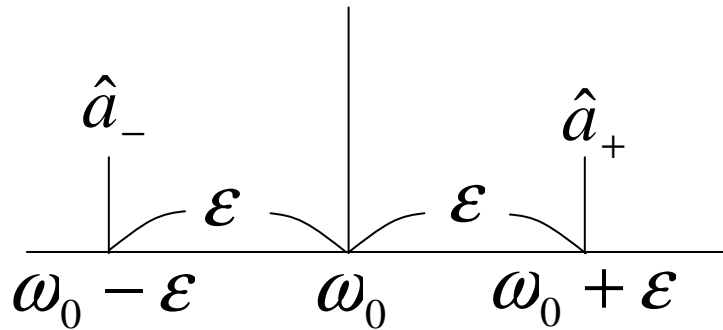


FIG. 3. (Color) Wigner function of the squeezed vacuum state produced by our OPO. The projections (solid curves) onto the two quadratures yield the Gaussian probability distributions with variances of -11.5 and 16 dB relative to the projections belonging to a pure vacuum state (dotted curves).

Two mode squeezed states(1): side-band squeezing



$$[\hat{a}_+, \hat{a}_+^\dagger] = [\hat{a}_-, \hat{a}_-^\dagger] = 1$$

$$[\hat{a}_+, \hat{a}_-^\dagger] = [\hat{a}_-, \hat{a}_+^\dagger] = 0$$

Quadrature-phase amplitudes can be defined by
(in photon-flux stance, Cook's claim)

$$\hat{\chi}_1 = \frac{1}{2} (\hat{a}_+ + \hat{a}_-^\dagger), \quad \hat{\chi}_2 = \frac{1}{2} (-i\hat{a}_+ + i\hat{a}_-^\dagger)$$

Note that these are not Hermitian

$$[\hat{\chi}_1, \hat{\chi}_2] = [\hat{\chi}_2, \hat{\chi}_1] = [\hat{\chi}_1, \hat{\chi}_1^\dagger] = [\hat{\chi}_2, \hat{\chi}_2^\dagger] = 0$$

$$[\hat{\chi}_2, \hat{\chi}_1^\dagger] = [\hat{\chi}_1, \hat{\chi}_2^\dagger] = \frac{i}{2}$$

Carlton M. Caves and Bonny L. Schumaker, "New formalism for two-photon quantum optics. I. Quadrature phases and squeezed states," Phys. Rev A31, 3068 (1985).

Bernard Yurke, "Squeezed-coherent-state generation via four-wave mixers and detection via homodyne detectors," Phys. Rev. A32, 300 (1985).

Two mode squeezed states (2)

Two-mode squeeze operator

$$\hat{S}(r, \varphi) \equiv \exp \left[r \left(\hat{a}_+ \hat{a}_- e^{-2i\varphi} - \hat{a}_+^\dagger \hat{a}_-^\dagger e^{2i\varphi} \right) \right]$$

$$\hat{S}^\dagger(r, \varphi) \hat{a}_\pm \hat{S}(r, \varphi) = \hat{a}_\pm \cosh r - \hat{a}_\mp^\dagger e^{i\varphi} \sinh r$$

when $\varphi = 0$, $\hat{S}^\dagger(r, 0) \hat{\chi}_1 \hat{S}(r, 0) = \hat{\chi}_1 e^{-r}$

$$\hat{S}^\dagger(r, 0) \hat{\chi}_2 \hat{S}(r, 0) = \hat{\chi}_2 e^{+r}$$

Two-mode coherent states

$$\hat{D}(\hat{a}_+, \alpha_+) \hat{D}(\hat{a}_-, \alpha_-) |0\rangle, \quad \hat{D}(\hat{a}, \alpha) = \exp(\alpha \hat{a}^\dagger - \alpha^* \hat{a})$$

Two-mode squeezed-coherent states $|\psi\rangle$

$$|\psi\rangle = \hat{S}(r, \varphi) \hat{D}(\hat{a}_+, \alpha_+) \hat{D}(\hat{a}_-, \alpha_-) |0\rangle$$

Two mode squeezed states (3)

Mean-square uncertainty of a non-Hermitian operator \hat{R}

$$\begin{aligned}\langle |\Delta R|^2 \rangle &= \left\langle \left(\hat{R} - \langle \hat{R} \rangle \right) \left(\hat{R}^\dagger - \langle \hat{R} \rangle^* \right) \right\rangle_{\text{sym}} \\ &= \langle \hat{R} \hat{R}^\dagger \rangle_{\text{sym}} - \langle \hat{R} \rangle \langle \hat{R}^\dagger \rangle, \quad \langle \hat{A} \hat{B} \rangle_{\text{sym}} = \langle \hat{A} \hat{B} + \hat{B} \hat{A} \rangle / 2\end{aligned}$$

Mean-square uncertainty of quadrature amplitudes

$$\langle |\Delta \chi_1|^2 \rangle = \frac{1}{2} \langle \hat{\chi}_1 \hat{\chi}_1^\dagger + \hat{\chi}_1^\dagger \hat{\chi}_1 \rangle - \langle \hat{\chi}_1 \rangle \langle \hat{\chi}_1^\dagger \rangle$$

$$\langle |\Delta \chi_2|^2 \rangle = \frac{1}{2} \langle \hat{\chi}_2 \hat{\chi}_2^\dagger + \hat{\chi}_2^\dagger \hat{\chi}_2 \rangle - \langle \hat{\chi}_2 \rangle \langle \hat{\chi}_2^\dagger \rangle$$

For $\alpha_+ = \alpha_- = 0$ and $\varphi = 0$,

$$\langle |\Delta \chi_1|^2 \rangle = \frac{1}{4} e^{-2r}, \quad \langle |\Delta \chi_2|^2 \rangle = \frac{1}{4} e^{-2r}$$

$$\langle |\Delta \chi_1|^2 \rangle^{1/2} \langle |\Delta \chi_2|^2 \rangle^{1/2} = \frac{1}{4}$$

Outline of the talk

- Introduction
- Quantization of the electromagnetic fields
- Quantum theory of light

Number states (single photon sources),

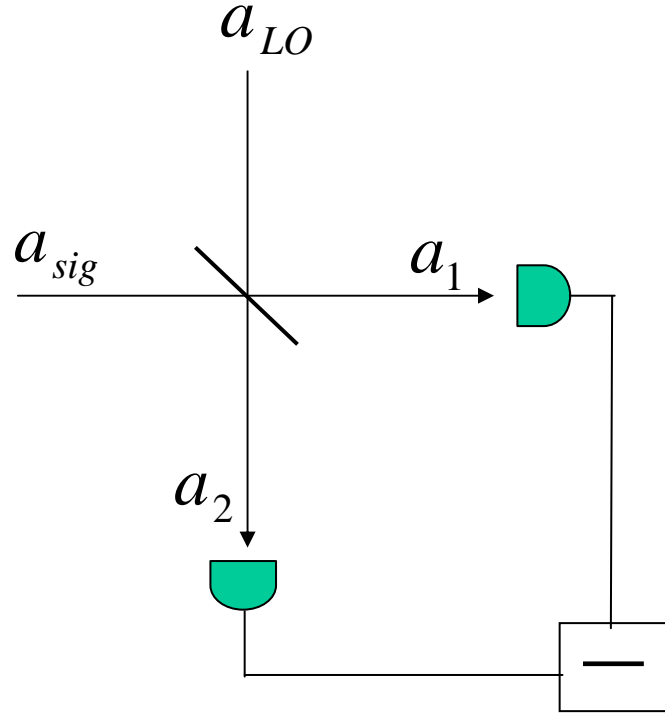
Coherent states,

Squeezed states,

Homodyne detection

- Nonlinear optics and Quantum state control
- Correlation function
- Representation of density matrix
- Precision measurements using atoms

Homodyne detection (1)



$$\begin{cases} \hat{a}_1 = \frac{1}{\sqrt{2}}(\hat{a}_{sig} + \hat{a}_{LO}) \\ \hat{a}_2 = \frac{1}{\sqrt{2}}(\hat{a}_{sig} - \hat{a}_{LO}) \end{cases}$$

$$\hat{n} = \hat{a}_1^\dagger \hat{a}_1 - \hat{a}_2^\dagger \hat{a}_2$$

$$= \hat{a}_{sig}^\dagger \hat{a}_{LO} + \hat{a}_{sig} \hat{a}_{LO}^\dagger$$

When LO is a bright coherent light, $a_{LO} \rightarrow \sqrt{n_{LO}} e^{i\theta}$

$$\hat{n} = 2\sqrt{n_{LO}} \left\{ \frac{\hat{a}_s + \hat{a}_s^\dagger}{2} \cos \theta + \frac{\hat{a}_s - \hat{a}_s^\dagger}{2i} \sin \theta \right\}$$

$$= 2\sqrt{n_{LO}} \{ \hat{x}_1 \cos \theta + \hat{x}_2 \sin \theta \}$$

Homodyne detection (2)

Multimode homodyne detection

$$a_1(\omega) = \frac{1}{\sqrt{2}}(a_s(\omega) + a_{\text{LO}}(\omega)), \quad a_2(\omega) = \frac{1}{\sqrt{2}}(a_s(\omega) - a_{\text{LO}}(\omega))$$

We assume that a photodiode measures photon flux:

$$I_1(t) = e \int_0^\infty d\omega \int_0^\infty d\omega' a_1^\dagger(\omega) a_1(\omega') e^{i(\omega-\omega')t} e^{-\left(\frac{\omega-\omega'}{B}\right)^2}$$

$$I_2(t) = e \int_0^\infty d\omega \int_0^\infty d\omega' a_2^\dagger(\omega) a_2(\omega') e^{i(\omega-\omega')t} e^{-\left(\frac{\omega-\omega'}{B}\right)^2}$$

where e is elementary charge, B is the bandwidth of PDs.

$$I(t) = I_1(t) - I_2(t)$$

$$= e \int_0^\infty d\omega \int_0^\infty d\omega' \{a_1^\dagger(\omega) a_1(\omega') - a_2^\dagger(\omega) a_2(\omega')\} e^{i(\omega-\omega')t} e^{-\left(\frac{\omega-\omega'}{B}\right)^2}$$

$$= e \int_0^\infty d\omega \int_0^\infty d\omega' \{a_{\text{LO}}^\dagger(\omega) a_s(\omega') + a_s^\dagger(\omega) a_{\text{LO}}(\omega')\} e^{i(\omega-\omega')t} e^{-\left(\frac{\omega-\omega'}{B}\right)^2}$$

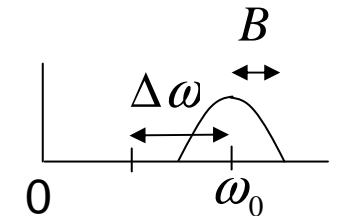
Homodyne detection (3)

We assume that the LO is in a monochromatic coherent state.

$$\begin{aligned}\hat{a}_{\text{LO}}(\omega)|\alpha_{\text{LO}}(\omega)\rangle &= \alpha_{\text{LO}}\delta(\omega - \omega_0)|\alpha_{\text{LO}}(\omega_0)\rangle \\ \langle\{\alpha_{\text{LO}}\}|I(t)|\{\alpha_{\text{LO}}\}\rangle &= e \int_0^\infty d\omega \int_0^\infty d\omega' \left\{ \alpha_{\text{LO}}^* \delta(\omega - \omega_0) a_s(\omega') + a_s^\dagger(\omega) \alpha_{\text{LO}} \delta(\omega' - \omega_0) \right\} \\ &\quad \times e^{i(\omega-\omega')t} e^{-\left(\frac{\omega-\omega'}{B}\right)^2} \\ &= e\sqrt{n_{\text{LO}}} \int_0^\infty d\omega \left\{ a_s(\omega) e^{-i\theta_{\text{LO}}} e^{-i(\omega-\omega_0)t} + a_s^\dagger(\omega) e^{i\theta_{\text{LO}}} e^{i(\omega-\omega_0)t} \right\} e^{-\left(\frac{\omega-\omega'}{B}\right)^2}\end{aligned}$$

chang of variable : $\varepsilon = \omega - \omega_0$, and take $\Delta\omega \gg B$.

$$\begin{aligned}&= e\sqrt{n_{\text{LO}}} \int_{-\Delta\omega}^{\Delta\omega} d\omega \left\{ a_s(\omega_0 + \varepsilon) e^{-i\theta_{\text{LO}}} e^{-i\varepsilon t} + a_s^\dagger(\omega_0 + \varepsilon) e^{i\theta_{\text{LO}}} e^{i\varepsilon t} \right\} e^{-\left(\frac{\varepsilon}{B}\right)^2} \\ &= e\sqrt{n_{\text{LO}}} \int_0^{\Delta\omega} d\omega \left\{ a_s(\omega_0 + \varepsilon) e^{-i\theta_{\text{LO}}} e^{-i\varepsilon t} + a_s^\dagger(\omega_0 + \varepsilon) e^{i\theta_{\text{LO}}} e^{i\varepsilon t} \right. \\ &\quad \left. + a_s(\omega_0 - \varepsilon) e^{-i\theta_{\text{LO}}} e^{i\varepsilon t} + a_s^\dagger(\omega_0 - \varepsilon) e^{i\theta_{\text{LO}}} e^{-i\varepsilon t} \right\} e^{-\left(\frac{\varepsilon}{B}\right)^2}\end{aligned}$$



Homodyne detection (4)

Using quadrature-phase amplitude, we obtain

$$\langle \{\alpha_{\text{LO}}\} | I(t) | \{\alpha_{\text{LO}}\} \rangle = 2e\sqrt{n_{\text{LO}}} \int_0^{\Delta\omega} d\omega e^{-\left(\frac{\varepsilon}{B}\right)^2} \{ \chi(\varepsilon, \theta_{\text{LO}}) e^{-i\varepsilon t} + \chi^\dagger(\varepsilon, \theta_{\text{LO}}) e^{i\varepsilon t} \}$$

where $\chi(\varepsilon, \theta) = \frac{1}{2} \{ a_s(\omega_0 + \varepsilon) e^{-i\theta} + a_s^\dagger(\omega_0 - \varepsilon) e^{i\theta} \}$

note $\chi^\dagger(\varepsilon, \theta) = \chi(-\varepsilon, \theta)$

Therefore, ε - frequency component of the deference current, $I(\varepsilon)$, is given by

$$I(\varepsilon) = 2e\sqrt{n_{\text{LO}}} e^{-\left(\frac{\varepsilon}{B}\right)^2} \{ \chi(\varepsilon, \theta_{\text{LO}}) e^{-i\varepsilon t} + \chi^\dagger(\varepsilon, \theta_{\text{LO}}) e^{i\varepsilon t} \}$$

Noise power measured by a spectrum analyzer $S(\varepsilon)$

\Rightarrow zero - frequency component of $I^2(\varepsilon)$ (video bandwidth)

$$S(\varepsilon) = 4e^2 n_{\text{LO}} e^{-\left(\frac{2\varepsilon}{B}\right)^2} \underbrace{\langle \chi(\varepsilon, \theta_{\text{LO}}) \chi^\dagger(\varepsilon, \theta_{\text{LO}}) + \chi^\dagger(\varepsilon, \theta_{\text{LO}}) \chi(\varepsilon, \theta_{\text{LO}}) \rangle}_{\text{Mean-square uncertainty of the quadrature amplitude}}$$

Mean-square uncertainty of the quadrature amplitude

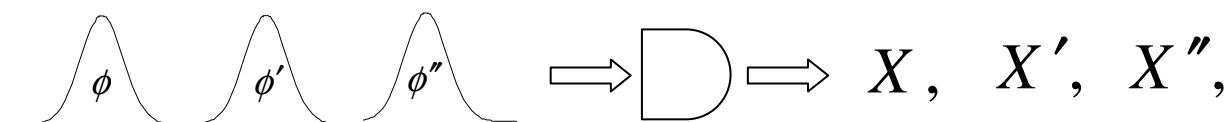
Pulsed homodyne detection

Pulsed homodyne detection differs from the usually-used method of using radio-frequency spectral analysis of the current to study noise at certain frequencies. In the pulsed homodyne detection, photoelectrons generated by each pulse are separately amplified by a low-noise amplifier, so a single measurement on the quadrature amplitude of the signal pulse is performed pulse by pulse.

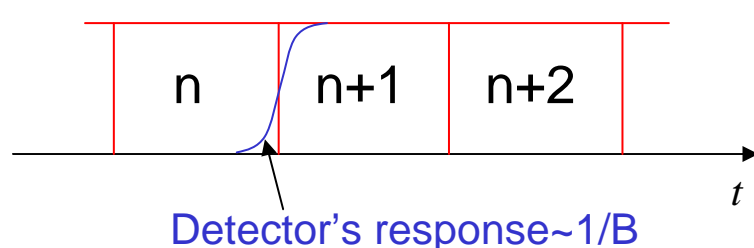
A charge sensitive amplifier: repetition freq. < 1MHz

ref. D.T.Smithey, M. Beck, M.G. Raymer, and A. Faridani, Phys. Rev. Lett. 70, 1244 (1992).

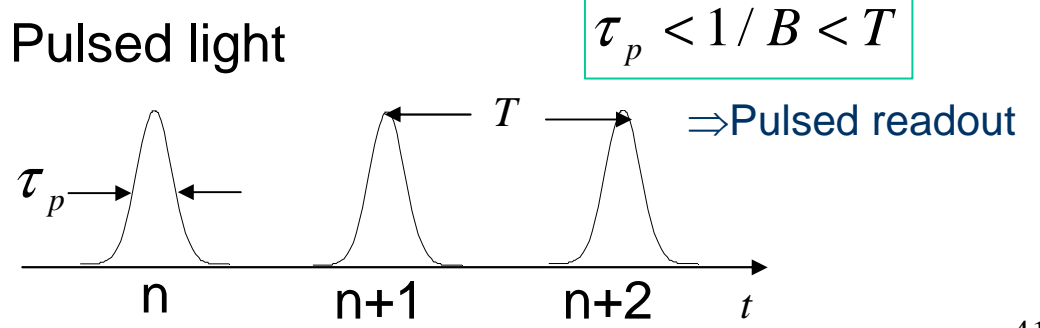
Now, using a low noise op-amp, repetition freq.~100MHz is possible.



continuous-wave

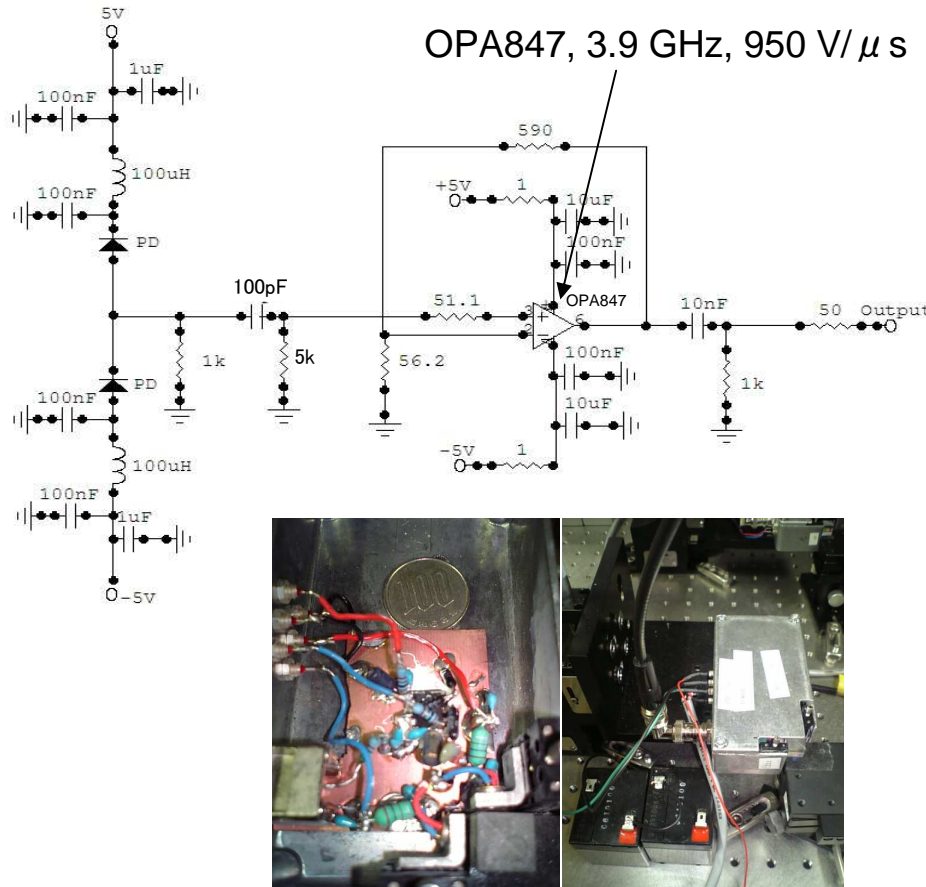


Pulsed light

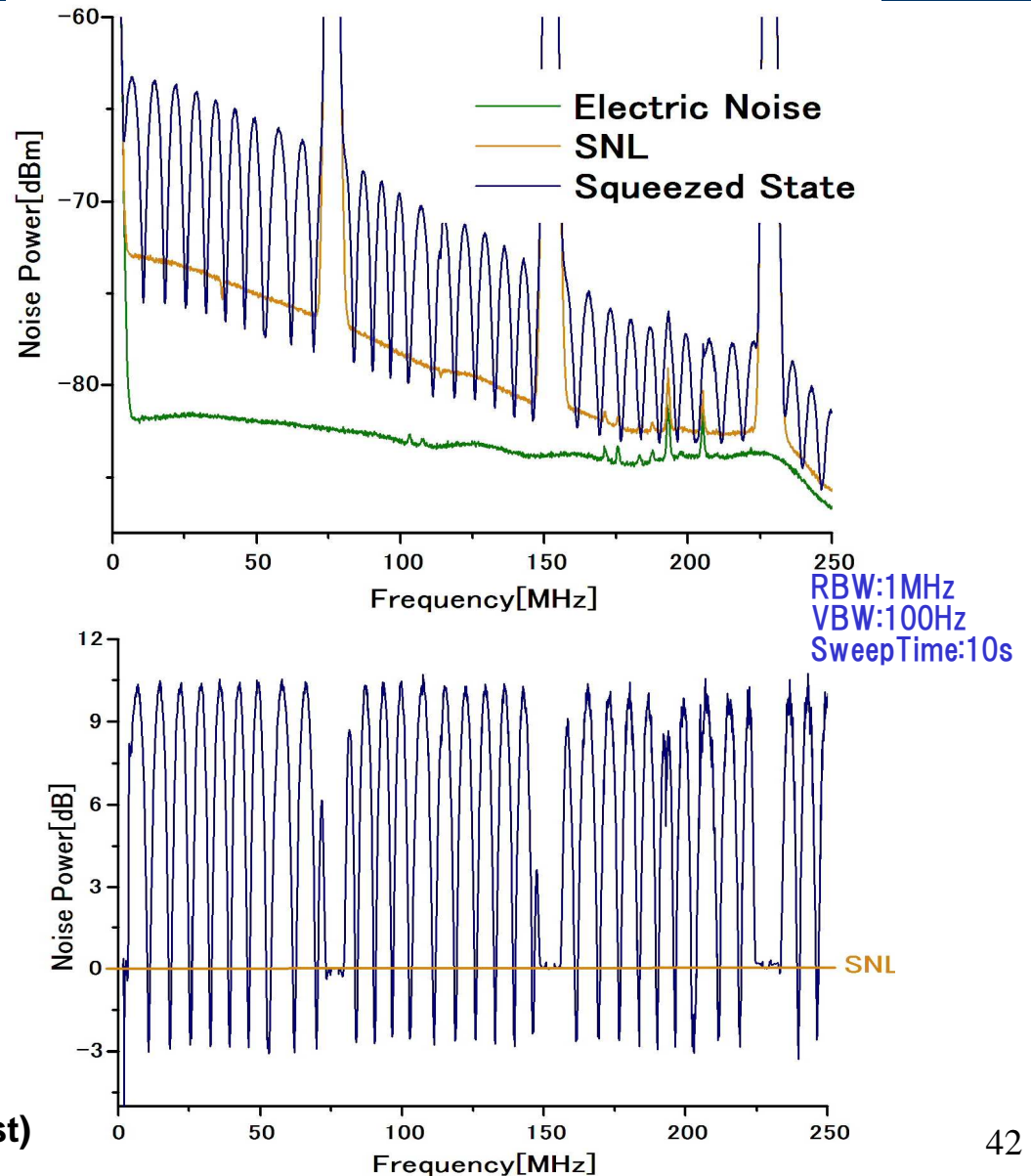


High speed homodyne detector made of OpAmp

Okubo *et al.*, Opt. Lett. 33, 1458 (2008).

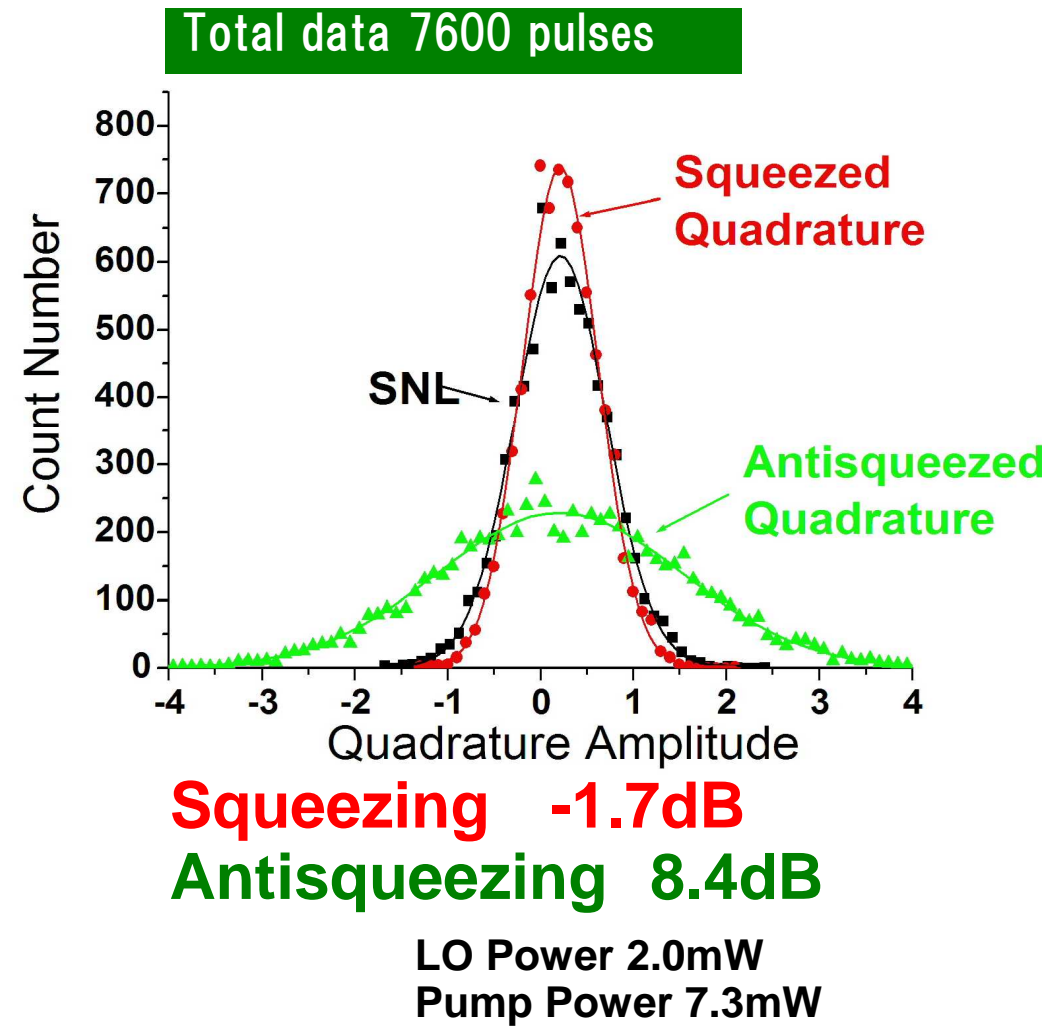
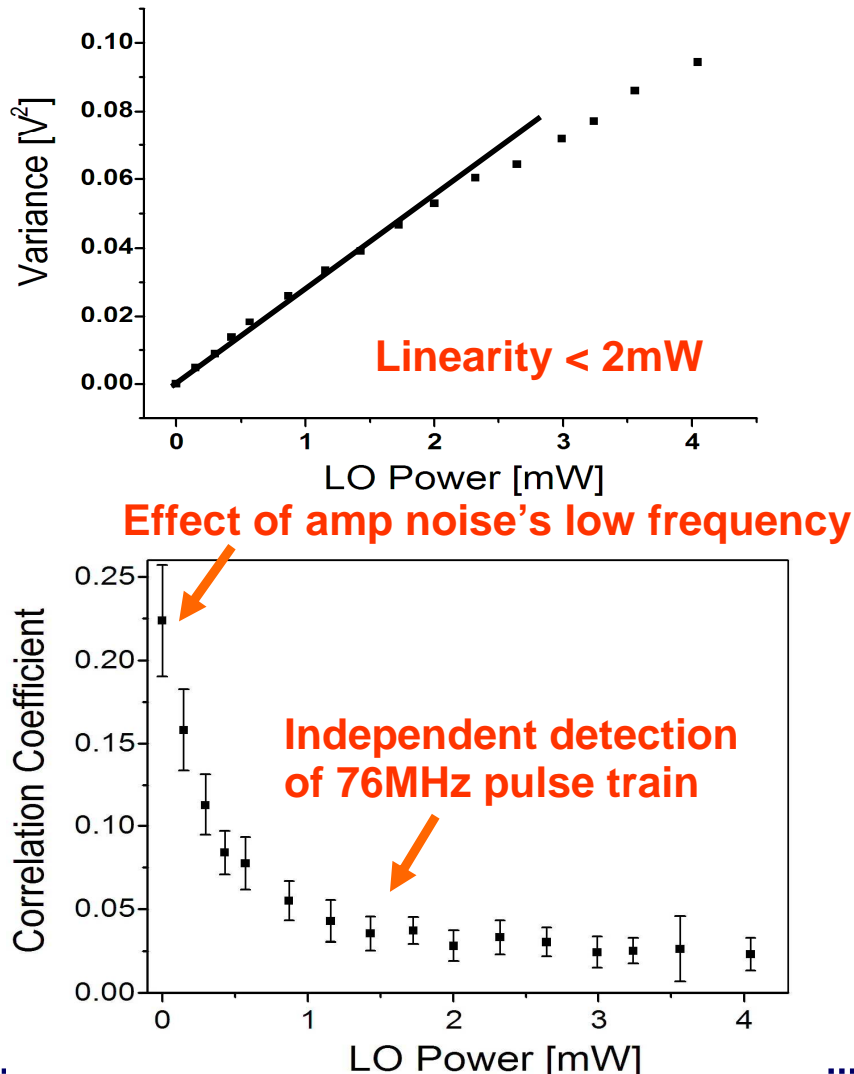


Useful bandwidth > 200MHz
Observation of squeezing over several rep. freq. (first)



Performance of detector and Measurement Squeezed states in time domain

Okubo *et al.*, Opt. Lett. 33, 1458 (2008).



- One point is an average of 10 measurements
- error bar is a standard deviation of 10 measurements

Correlation coefficient of adjacent squeezed pulse is 0.04

Outline of the talk

- Introduction
- Quantization of the electromagnetic fields
- Quantum theory of light

Number states (single photon sources),
Coherent states,
Squeezed states,
Homodyne detection

- Nonlinear optics and Quantum state control
- Correlation function
- Representation of density matrix
- Precision measurements using atoms

Nonlinear optics and Quantum state control

Electric field and dielectric polarization:

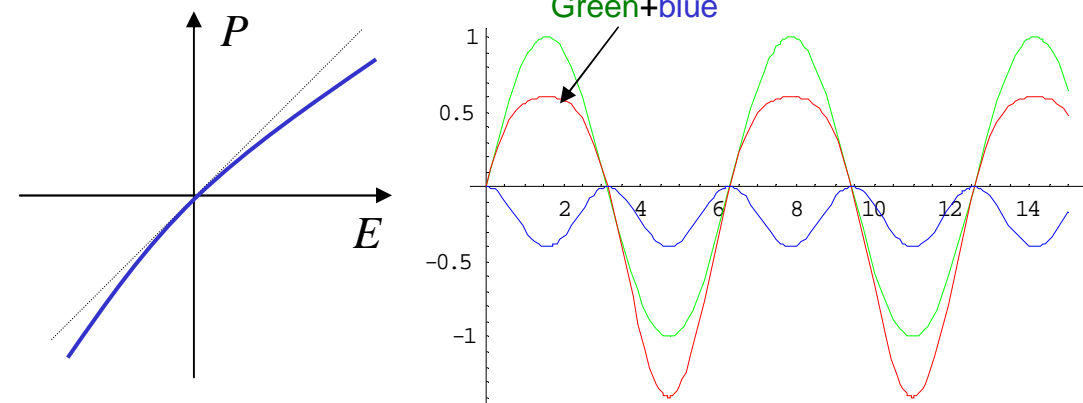
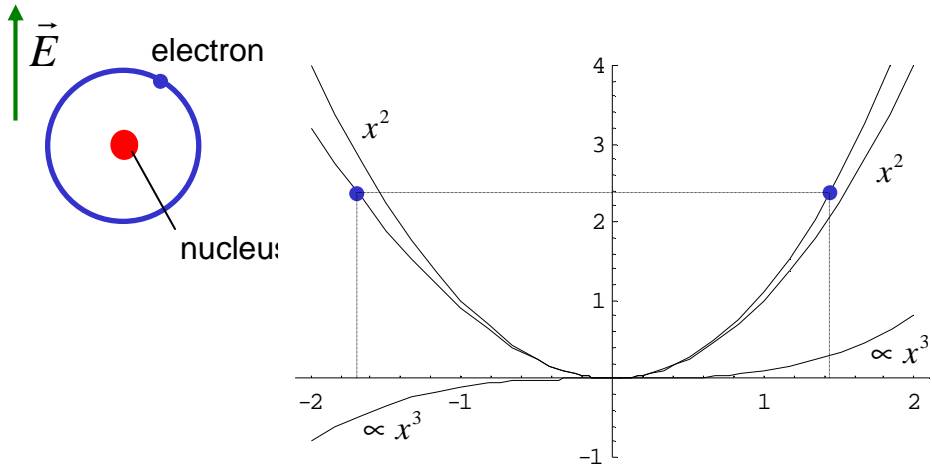
$$\vec{D}(\vec{r}, t) = \epsilon_0 \vec{E}(\vec{r}, t) + \vec{P}(\vec{r}, t)$$

The polarization may be written as a power series:

$$\vec{P} = \epsilon_0 \chi_E \vec{E} + \epsilon_0 \chi^{(2)} : \vec{E} \vec{E} + \epsilon_0 \chi^{(3)} : \vec{E} \vec{E} \vec{E} + \dots$$

(This is not the case for an extremely high electric field.)

Intuitive picture of dielectric polarization:



Nonlinear optics and quantum state control (2)

Second order nonlinear polarization:

$$(\vec{P}_{NL}^{(2)})_i = 2\epsilon_0 d_{ijk}^{(2)} E_j E_k$$

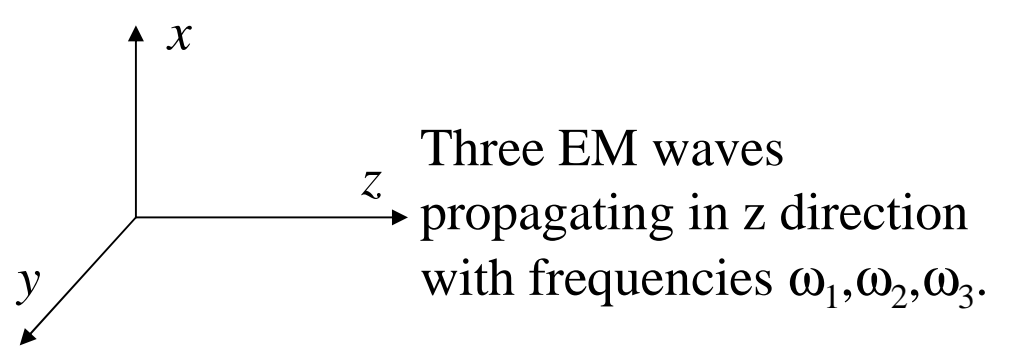
$$\text{rot } \vec{H} = \frac{\partial \vec{D}}{\partial t} + \vec{i}$$

$$\begin{aligned} &= \frac{\partial}{\partial t} (\epsilon_0 \vec{E} + \epsilon_0 \chi_e \vec{E} + \vec{P}_{NL}) + \sigma \vec{E} \\ &= \frac{\partial}{\partial t} (\epsilon \vec{E}) + \frac{\partial}{\partial t} \vec{P}_{NL} + \sigma \vec{E} \end{aligned}$$

$$\text{rot} \left(\text{rot} \vec{E} + \frac{\partial \vec{B}}{\partial t} \right) = 0$$

$$-\nabla^2 \vec{E} + \mu_0 \frac{\partial}{\partial t} \text{rot} \vec{H} = 0 \quad \text{(magnetic polarization ignored)}$$

$$\nabla^2 \vec{E} = \mu_0 \epsilon \frac{\partial^2}{\partial t^2} \vec{E} + \mu_0 \frac{\partial^2}{\partial t^2} \vec{P}_{NL} + \mu_0 \sigma \frac{\partial \vec{E}}{\partial t}$$



Three EM waves propagating in z direction with frequencies $\omega_1, \omega_2, \omega_3$.

$$\left\{ \begin{array}{l} E_i^{(\omega_1)}(z, t) = 1/2(E_{1i}(z)e^{i(\omega_1 t - k_1 z)} + \text{c.c.}) \\ E_j^{(\omega_2)}(z, t) = 1/2(E_{2j}(z)e^{i(\omega_2 t - k_2 z)} + \text{c.c.}) \\ E_k^{(\omega_3)}(z, t) = 1/2(E_{3k}(z)e^{i(\omega_3 t - k_3 z)} + \text{c.c.}) \end{array} \right.$$

Nonlinear polarization at frequency $\omega_1 = \omega_3 - \omega_2$

$$\begin{aligned} (\vec{P}_{NL}^{(\omega_1)}(z, t))_i &= 2\epsilon_0 d_{ijk} E_j^{(\omega_2)} E_k^{(\omega_3)} \\ &= \frac{1}{2} \epsilon_0 d_{ijk} E_{2j}^*(z) E_{3k}(z) e^{i(\omega_{23} - \omega_2)t - i(k_3 - k_2)z} + \text{c.c.} \end{aligned}$$

Nonlinear optics and quantum state control (3)

$$\begin{aligned}
\nabla^2 E_i^{(\omega_1)}(z, t) &= \frac{1}{2} \left\{ \frac{\partial^2}{\partial z^2} \left(E_{1i}(z) e^{i(\omega_1 t - k_1 z)} \right) + \text{c.c} \right\} \\
&= \frac{1}{2} \left\{ \frac{\partial^2}{\partial z^2} \left(E_{1i}(z) e^{i(\omega_1 t - k_1 z)} \right) + \text{c.c} \right\} \\
&= \frac{1}{2} \left\{ \left(\frac{\partial^2 E_{1i}(z)}{\partial z^2} - 2ik_1 \frac{\partial E_{1i}(z)}{\partial z} - k_1^2 E_{1i}(z) \right) e^{i(\omega_1 t - k_1 z)} + \text{c.c} \right\}
\end{aligned}$$

Slowly varying amplitude approximation

$$\left| \frac{\partial^2 E_{1i}(z)}{\partial z^2} \right| \ll \left| k_1 \frac{\partial E_{1i}(z)}{\partial z} \right| \quad k = \frac{2\pi}{\lambda}$$

$$\nabla^2 E_i^{(\omega_1)}(z, t) \approx \frac{1}{2} \left\{ \left(-2ik_1 \frac{\partial E_{1i}(z)}{\partial z} - k_1^2 E_{1i}(z) \right) e^{i(\omega_1 t - k_1 z)} + \text{c.c} \right\}$$

$$= \left\{ \mu_0 \epsilon_1(-\omega_1^2) + i\omega_1 \mu_1 \sigma_1 \right\} \left\{ \frac{1}{2} E_{1i} e^{i(\omega_1 t - k_1 z)} + \text{c.c.} \right\} + \mu_0 \frac{\partial^2}{\partial t^2} \left(P_{NL}^{\omega_1} \right)_i$$

Nonlinear optics and quantum state control (3)

$$\begin{aligned}
\nabla^2 E_i^{(\omega_1)}(z, t) &= \frac{1}{2} \left\{ \frac{\partial^2}{\partial z^2} \left(E_{1i}(z) e^{i(\omega_1 t - k_1 z)} \right) + \text{c.c} \right\} \\
&= \frac{1}{2} \left\{ \frac{\partial^2}{\partial z^2} \left(E_{1i}(z) e^{i(\omega_1 t - k_1 z)} \right) + \text{c.c} \right\} \\
&= \frac{1}{2} \left\{ \left(\frac{\partial^2 E_{1i}(z)}{\partial z^2} - 2ik_1 \frac{\partial E_{1i}(z)}{\partial z} - k_1^2 E_{1i}(z) \right) e^{i(\omega_1 t - k_1 z)} + \text{c.c} \right\}
\end{aligned}$$

Slowly varying amplitude approximation

$$\begin{aligned}
\left| \frac{\partial^2 E_{1i}(z)}{\partial z^2} \right| &\ll \left| k_1 \frac{\partial E_{1i}(z)}{\partial z} \right| \quad k = \frac{2\pi}{\lambda} \\
\nabla^2 E_i^{(\omega_1)}(z, t) &\approx \frac{1}{2} \left\{ \left(-2ik_1 \frac{\partial E_{1i}(z)}{\partial z} - k_1^2 E_{1i}(z) \right) e^{i(\omega_1 t - k_1 z)} + \text{c.c} \right\} \\
&= \left\{ \mu_0 \epsilon_1(-\omega_1^2) + i\omega_1 \mu_1 \sigma_1 \right\} \left\{ \frac{1}{2} E_{1i} e^{i(\omega_1 t - k_1 z)} + \text{c.c.} \right\} + \mu_0 \frac{\partial^2}{\partial t^2} \left(P_{NL}^{\omega_1} \right)_i
\end{aligned}$$

Nonlinear optics and quantum state control (4)

$$\left\{ \begin{array}{l} \frac{dA_1}{dz} = -\frac{\alpha_1}{2} A_1 - i\beta A_2^* A_3 e^{-i\Delta kz} \\ \frac{dA_2}{dz} = -\frac{\alpha_2}{2} A_2 - i\beta A_1^* A_3 e^{-i\Delta kz} \\ \frac{dA_3}{dz} = -\frac{\alpha_3}{2} A_3 - i\beta A_1 A_2 e^{i\Delta kz} \end{array} \right.$$

$$A_l = \sqrt{\frac{n_l}{\omega_l}} E_l, \quad \alpha_l = \sigma_l \sqrt{\frac{\mu_0}{\epsilon_l}}, \quad \Delta k = k_3 - k_1 - k_2$$

$$\beta = \frac{d_{ijk}}{2} \frac{\epsilon_l \mu_0 \omega_l^2}{k_l} \sqrt{\frac{n_1 \omega_2 \omega_3}{\omega_1 n_2 n_3}} = \frac{d_{ijk}}{2c} \sqrt{\frac{\omega_1 \omega_2 \omega_3}{n_1 n_2 n_3}}$$

Second harmonic generation

$$\omega_1 = \omega_2 \quad (A_1 = A_2), \quad \sigma_l = 0 \quad (\text{lossless})$$

$$\left\{ \begin{array}{l} \frac{dA_1}{dz} = -i\beta A_1^* A_3 e^{-i\Delta kz} \\ \frac{dA_3}{dz} = -i\beta A_1^2 e^{i\Delta kz} \end{array} \right.$$

$$\frac{d}{dz} (|A_1|^2 + |A_3|^2) = 0$$

Energy conservation

When $|A_1| \ll |A_3|$, $A_1 \approx \text{const.}$ $A_3(0) = 0$

$$A_3(z) = -i\beta A_1^2 \frac{e^{i\Delta kz} - 1}{i\Delta k}$$

$$|A_3(z)| = |\beta|^2 |A_1|^4 \frac{\sin^2(\Delta kz / 2)}{(\Delta k / 2)^2}$$

if $\Delta k = 0$

$$|A_3(z)| = |\beta|^2 |A_1|^4 z^2$$

Parametric process

$$\omega_1 = \omega_2 \quad (A_1 = A_2, \omega_3 = 2\omega_1), \quad \sigma_l = 0 \quad (\text{lossless})$$

When $|A_1| \ll |A_3|$, $A_3 \approx \text{const.}$ $A_3(0) = 0$

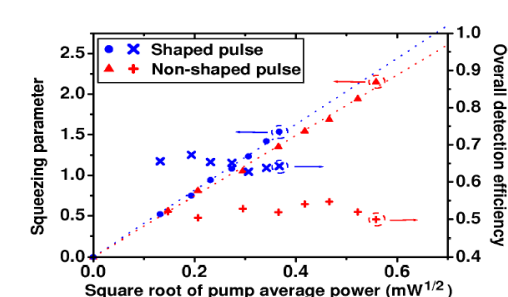
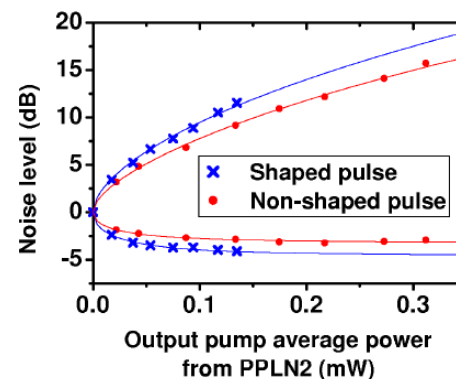
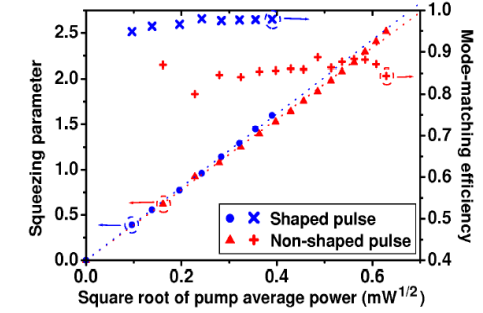
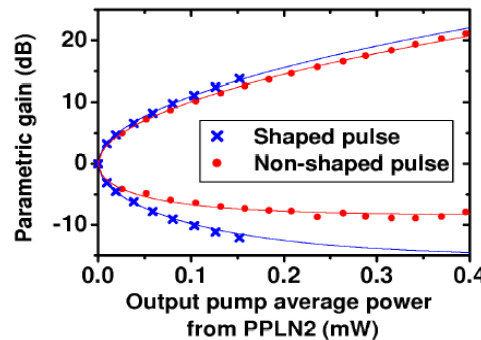
$$\begin{aligned} \frac{dA_1}{dz} &= -i\beta A_1^* A_3 e^{-i\Delta kz} \\ &= -gA_1^* e^{-i\Delta kz + i\varphi} \quad ge^{i\varphi} = i\beta A_3 \end{aligned}$$

$$\rightarrow \frac{d^2 A_1}{dz^2} = g^2 A_1$$

$$A_1(z) = C_1 e^{gz} + C_2 e^{-gz}$$

$$\therefore A_1(z) = A_1(0) \cosh gz - A_1^*(0) e^{i\varphi} \sinh gz$$

$$\text{note} \quad \hat{S}^\dagger(\zeta) \hat{a} \hat{S}(\zeta) = \hat{a} \cosh r - \hat{a}^\dagger e^{i\varphi} \sinh r$$



$$S_{\pm} = \eta \exp(\pm 2r) + 1 - \eta.$$

Outline of the talk

- Introduction
- Quantization of the electromagnetic fields
- Quantum theory of light

Number states (single photon sources),
Coherent states,
Squeezed states,
Homodyne detection

- Nonlinear optics and Quantum state control
- Correlation function
- Representation of density matrix
- Precision measurements using atoms

Correlation functions

One photon detection probability

$$\hat{E}_{\vec{k},\sigma}(\vec{r},t) = \hat{E}_{\vec{k},\sigma}^{(+)}(\vec{r},t) + \hat{E}_{\vec{k},\sigma}^{(-)}(\vec{r},t)$$

$$\hat{E}_{\vec{k},\sigma}^{(+)}(\vec{r},t) = i \sqrt{\frac{\hbar \omega_k}{2 \epsilon_0 V}} \hat{a}_{\vec{k},\sigma} \exp(-i \omega_k t + i \vec{k} \cdot \vec{r})$$

$|i\rangle \rightarrow |f\rangle$: one photon in mode \vec{k} , σ is annihilated.

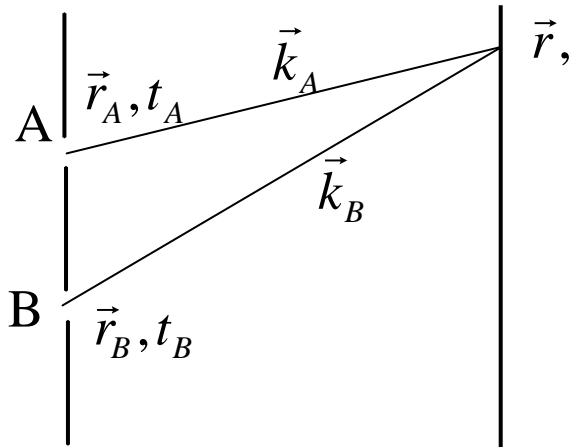
$$\begin{aligned} P^{(1)} &= \sum_f K \left| \langle f | \hat{E}_{\vec{k},\sigma}^{(+)} | i \rangle \right|^2 = K \sum_f \left| \langle f | \hat{E}_{\vec{k},\sigma}^{(+)} | i \rangle \right|^2 = K \sum_f \langle i | \hat{E}_{\vec{k},\sigma}^{(-)} | f \rangle \langle f | \hat{E}_{\vec{k},\sigma}^{(+)} | i \rangle \\ &= K \langle i | \hat{E}_{\vec{k},\sigma}^{(-)} \hat{E}_{\vec{k},\sigma}^{(+)} | i \rangle \end{aligned}$$

when one photon in mode \vec{k} , σ , another one photon in mode \vec{k}' , σ' are annihilated.

$$\begin{aligned} P^{(2)} &= \sum_f K \left| \langle f | \hat{E}_{\vec{k},\sigma}^{(+)} \hat{E}_{\vec{k}',\sigma'}^{(+)} | i \rangle \right|^2 = K \sum_f \langle i | \hat{E}_{\vec{k}',\sigma'}^{(-)} \hat{E}_{\vec{k},\sigma}^{(-)} | f \rangle \langle f | \hat{E}_{\vec{k},\sigma}^{(+)} \hat{E}_{\vec{k}',\sigma'}^{(+)} | i \rangle \\ &= K \langle i | \hat{E}_{\vec{k}',\sigma'}^{(-)} \hat{E}_{\vec{k},\sigma}^{(-)} \hat{E}_{\vec{k},\sigma}^{(+)} \hat{E}_{\vec{k}',\sigma'}^{(+)} | i \rangle \end{aligned}$$

The first order correlation function (1)

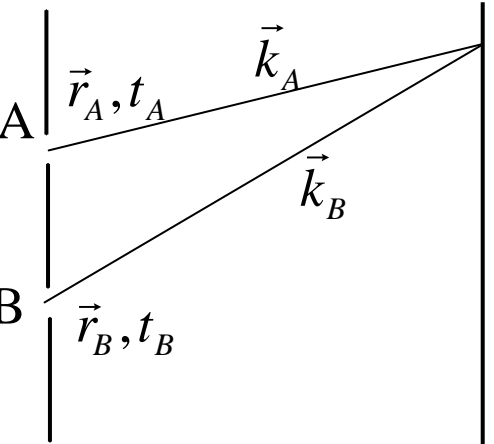
$$g^{(1)}(\vec{r}_A, t_A, \vec{r}_B, t_B) = \frac{\langle \hat{E}^{(-)}(\vec{r}_A, t_A) \hat{E}^{(+)}(\vec{r}_B, t_B) \rangle}{\langle \hat{E}^{(-)}(\vec{r}_A, t_A) \hat{E}^{(+)}(\vec{r}_A, t_A) \rangle^{1/2} \langle \hat{E}^{(-)}(\vec{r}_B, t_B) \hat{E}^{(+)}(\vec{r}_B, t_B) \rangle^{1/2}}$$



$$\begin{aligned} \hat{E}^{(+)}(\vec{r}_A, t_A) &= i \sqrt{\frac{\hbar \omega_k}{2 \epsilon_0 V}} \hat{a}_A \exp(-i \omega t_A + i \vec{k}_A \cdot \vec{r}_A) \\ &= i \sqrt{\frac{\hbar \omega_k}{2 \epsilon_0 V}} \hat{a}_A \exp(-i \omega t + i \vec{k}_A \cdot \vec{r}) \\ &= \hat{E}_A^{(+)}(\vec{r}, t) \quad t_A = t - |\vec{r} - \vec{r}_A|/c \\ \hat{E}^{(+)}(\vec{r}_B, t_B) &= i \sqrt{\frac{\hbar \omega}{2 \epsilon_0 V}} \hat{a}_B \exp(-i \omega t_B + i \vec{k}_B \cdot \vec{r}_B) \\ &= i \sqrt{\frac{\hbar \omega}{2 \epsilon_0 V}} \hat{a}_B \exp(-i \omega t + i \vec{k}_B \cdot \vec{r}) \\ &= \hat{E}_B^{(+)}(\vec{r}, t) \end{aligned}$$

The first order correlation function (2)

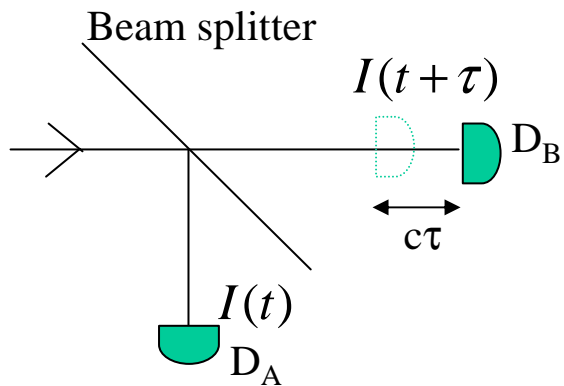
$$g^{(1)}(\vec{r}_A, t_A, \vec{r}_B, t_B) = \frac{\langle \hat{E}^{(-)}(\vec{r}_A, t_A) \hat{E}^{(+)}(\vec{r}_B, t_B) \rangle}{\langle \hat{E}^{(-)}(\vec{r}_A, t_A) \hat{E}^{(+)}(\vec{r}_A, t_A) \rangle^{1/2} \langle \hat{E}^{(-)}(\vec{r}_B, t_B) \hat{E}^{(+)}(\vec{r}_B, t_B) \rangle^{1/2}}$$

	<p>$\hat{E}^{(+)}(\vec{r}, t) = \hat{E}_A^{(+)}(\vec{r}, t) + \hat{E}_B^{(+)}(\vec{r}, t)$</p> <p>$P^{(1)}(\vec{r}, t) = K \langle \hat{E}^{(-)}(\vec{r}, t) \hat{E}^{(+)}(\vec{r}, t) \rangle$</p> $= K \left\{ \langle \hat{E}_A^{(-)} \hat{E}_A^{(+)} \rangle + \langle \hat{E}_B^{(-)} \hat{E}_B^{(+)} \rangle + \sqrt{AB} g^{(1)} + \sqrt{AB} g^{(1)\dagger} \right\}$ <p>$g^{(1)} = \begin{cases} 1 & \text{first - order coherent} \\ < 1 & \text{partial coherent} \\ 0 & \text{incoherent} \end{cases}$</p>
---	--

The second order correlation function (1)

$$g^{(2)}(\vec{r}_A, t_A, \vec{r}_B, t_B) = \frac{\langle \hat{E}^{(-)}(\vec{r}_A, t_A) \hat{E}^{(-)}(\vec{r}_B, t_B) \hat{E}^{(+)}(\vec{r}_B, t_B) \hat{E}^{(+)}(\vec{r}_A, t_A) \rangle}{\langle \hat{E}^{(-)}(\vec{r}_A, t_A) \hat{E}^{(+)}(\vec{r}_A, t_A) \rangle \langle \hat{E}^{(-)}(\vec{r}_B, t_B) \hat{E}^{(+)}(\vec{r}_B, t_B) \rangle}$$

second order autocorrelation function



$$g^{(2)}(\tau) = \frac{\langle \hat{E}^{(-)}(t) \hat{E}^{(-)}(t + \tau) \hat{E}^{(+)}(t + \tau) \hat{E}^{(+)}(t) \rangle}{\langle \hat{E}^{(-)}(t) \hat{E}^{(+)}(t) \rangle \langle \hat{E}^{(-)}(t + \tau) \hat{E}^{(+)}(t + \tau) \rangle}$$

Classical theory

$$g_C^{(2)}(\tau) = \frac{\langle I(t) I(t + \tau) \rangle}{\langle I(t) \rangle \langle I(t + \tau) \rangle}$$

$$g_C^{(2)}(0) = \frac{\langle I^2(t) \rangle}{\langle I(t) \rangle^2} = \frac{\langle (I(t) - \langle I(t) \rangle)^2 \rangle}{\langle I(t) \rangle^2} + \frac{\langle I(t) \rangle^2}{\langle I(t) \rangle^2} \geq 1$$

$$\lim_{\tau \rightarrow \infty} g_C^{(2)}(\tau) = 1 \quad (\because \langle I(t) I(t + \tau) \rangle \xrightarrow[\tau \rightarrow \infty]{} \langle I(t) \rangle \langle I(t + \tau) \rangle)$$

The second order correlation function (2)

Quantum theory

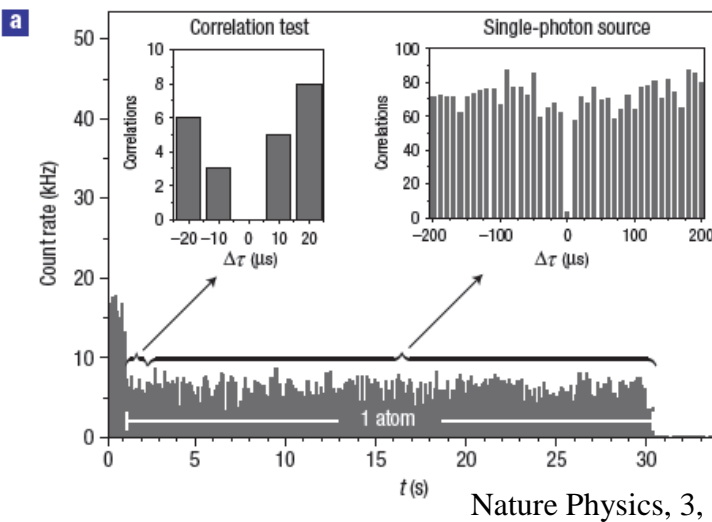
$$g^{(2)}(0) = \frac{\langle \hat{a}^{\dagger 2} \hat{a}^2 \rangle}{\langle \hat{a}^{\dagger} \hat{a} \rangle^2}$$

Fock states

$$\langle n | \hat{a}^{\dagger 2} \hat{a}^2 | n \rangle = n(n-1)$$

$$g^{(2)}(0) = \begin{cases} 0 & (n=0) \\ 1 - 1/n & (n \geq 1) \end{cases}$$

$$g^{(2)}(0) < 1 \text{ antibunching}$$



Coherent states

$$g^{(2)}(0) = 1 \quad g^{(n)}(0) = \frac{\langle \hat{a}^{\dagger n} \hat{a}^n \rangle}{\langle \hat{a}^{\dagger} \hat{a} \rangle^2} = 1$$

Squeezed states

$$g^{(2)}(0) = 1 + \frac{|\alpha|^2 \{ (e^{4r} - e^{2r}) \sin^2(\varphi - \theta/2) + (e^{-4r} - e^{-2r}) \cos^2(\varphi - \theta/2) \} + \sinh^2 r + 2 \sinh^4 r}{|\alpha|^2 \{ e^{2r} \sin^2(\varphi - \theta/2) + e^{-2r} \cos^2(\varphi - \theta/2) \} + \sinh^2 r}$$

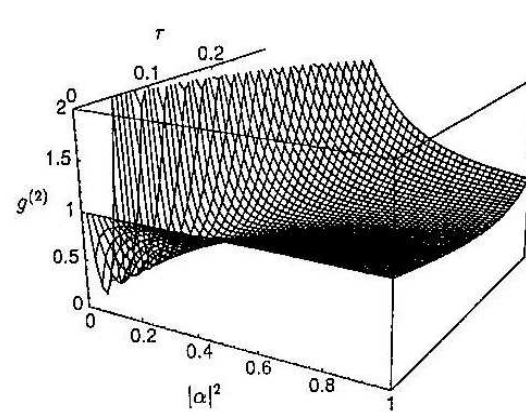
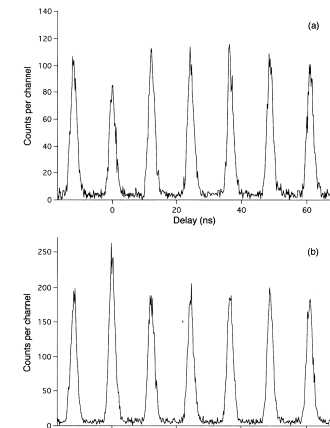


Fig.5 Normalized intensity correlation as a function of $|\alpha|^2$ and r for $\varphi = 0$.



Koashi, et al. PRL 71, 1164 (1993).

Thermal light

$$g^{(2)}(0) = 2 \quad P_n = \frac{\bar{n}^n}{(1 + \bar{n})^{n+1}}$$

Representation of density matrix (1)

Representation in Fock state basis

$$\begin{aligned}\hat{\rho} &= \sum_n \sum_m |n\rangle\langle n| \hat{\rho} |m\rangle\langle m| \\ &= \sum_n \sum_m \rho_{nm} |n\rangle\langle m|, \quad \rho_{nm} = \langle n|\hat{\rho}|m\rangle\end{aligned}$$

Example :coherent state

$$\hat{\rho} = |\alpha\rangle\langle\alpha| \quad \rho_{nm} = e^{-|\alpha|^2} \frac{\alpha^n \alpha^{*m}}{\sqrt{n!m!}}$$

Representation in coherent state basis ? Yes.

$$\begin{aligned}|\langle\alpha|\beta\rangle|^2 &= e^{-|\alpha-\beta|^2} \\ \int |\alpha\rangle\langle\alpha| d^2\alpha &= \sum_{n=0}^{\infty} \sum_{m=0}^{\infty} \frac{|n\rangle\langle m|}{\sqrt{n!m!}} \int e^{-|\alpha|^2} \alpha^n \alpha^{*m} d^2\alpha \\ &= \sum_{n=0}^{\infty} \frac{|n\rangle\langle m|}{n!} \pi n! = \pi \quad \text{coherent states are overcomplete.}\end{aligned}$$

Representation of density matrix (2)

Glauber-Sudarshan P-representation

$$\hat{\rho} = \int d^2\alpha P(\alpha) |\alpha\rangle\langle\alpha|$$

Expectation value of normally ordered operators

$$\begin{aligned}
 \langle \hat{a}^{\dagger n} \hat{a}^m \rangle &= \text{Tr}(\hat{\rho} \hat{a}^{\dagger n} \hat{a}^m) = \text{Tr}\left(\int d^2\alpha P(\alpha) |\alpha\rangle\langle\alpha| \hat{a}^{\dagger n} \hat{a}^m\right) = \text{Tr}\left(\int d^2\alpha P(\alpha) \langle\alpha|\hat{a}^{\dagger n} \hat{a}^m|\alpha\rangle\right) \\
 &= \int d^2\alpha P(\alpha) \alpha^{*n} \alpha^m \quad \hat{a}^\dagger \Rightarrow \alpha^*, \hat{a} \Rightarrow \alpha \\
 (\Delta x_1)^2 &= \langle x_1^2 \rangle - \langle x_1 \rangle^2 = \left\langle \frac{\hat{a}^2 + 2\hat{a}^\dagger \hat{a} + \hat{a}^{*\dagger} + 1}{4} \right\rangle - \left\langle \frac{\hat{a} + \hat{a}^\dagger}{2} \right\rangle^2 \\
 &= \frac{1}{4} \int d^2\alpha P(\alpha) \left\{ \alpha^2 + 2\alpha\alpha^* + \alpha^{*2} + 1 - (\alpha + \alpha^*)^2 \right\} \\
 &= \frac{1}{4} \left\{ 1 + \int d^2\alpha P(\alpha) [(\alpha + \alpha^*) - (\langle\alpha\rangle + \langle\alpha^*\rangle)]^2 \right\} \\
 (\Delta x_2)^2 &= \frac{1}{4} \left\{ 1 + \int d^2\alpha P(\alpha) \left[\left(\frac{\alpha - \alpha^*}{i} \right) - \left(\frac{\langle\alpha\rangle - \langle\alpha^*\rangle}{i} \right) \right]^2 \right\}
 \end{aligned}$$

$$\left\{ \begin{array}{l} \langle\alpha\rangle = \int d^2\alpha P(\alpha)\alpha \\ \langle\alpha^*\rangle = \int d^2\alpha P(\alpha)\alpha^* \end{array} \right.$$

if $P(\alpha) \geq 0$,

$$(\Delta x_1)^2 \geq \frac{1}{4} \text{ and } (\Delta x_2)^2 \geq \frac{1}{4}$$

Representation of density matrix (3)

$$\begin{aligned} (\Delta n)^2 &= \langle n^2 \rangle - \langle n \rangle^2 \\ &= \langle n \rangle + \int d^2 \alpha P(\alpha) \left[|\alpha|^2 - \langle |\alpha|^2 \rangle \right]^2 \end{aligned}$$

if $P(\alpha) \geq 0$, $(\Delta n)^2 \geq \langle n \rangle$

classical light : $P(\alpha) \geq 0$

Normally ordered characteristic function:

$$\begin{aligned} \chi_N(\eta) &= \text{Tr} \left(\hat{\rho} e^{\eta \hat{a}^\dagger} e^{-\eta^* \hat{a}} \right) \\ &= \int d^2 \alpha P(\alpha) e^{\eta \alpha^*} e^{-\eta^* \alpha} \end{aligned}$$

$$\eta = x_\eta + iy_\eta, \quad \alpha = x_\alpha + iy_\alpha$$

$$\chi_N(\eta) = \int d^2 \alpha P(\alpha) e^{2iy_\eta x_\alpha} e^{-2ix_\eta y_\alpha}$$

$$\chi_N(\eta) = \mathcal{F}\{P(\alpha/2)\}$$

$$P(\alpha/2) = \mathcal{F}^{-1}\{\chi_N(\eta)\}$$

Wigner distribution function:

$$\begin{aligned} \chi(\eta) &= \text{Tr} \left(\hat{\rho} e^{\eta \hat{a}^\dagger - \eta^* \hat{a}} \right) = \chi_N(\eta) e^{-|\eta|^2/2} \\ W(\alpha) &\equiv \int d^2 \eta \chi(\eta) e^{\eta^* \alpha - \eta \alpha^*} \\ &= \int d^2 \eta \chi_N(\eta) e^{-|\eta|^2/2} e^{\eta^* \alpha - \eta \alpha^*} \\ &= \frac{2}{\pi} \int d^2 \beta P(\beta) e^{-2|\beta - \alpha|^2} \end{aligned}$$

Example :coherent state

$$\begin{aligned} W(\alpha) &= \frac{2}{\pi} \int d^2 \beta \delta^{(2)}(\beta - \alpha_0) e^{-2|\beta - \alpha|^2} \\ &= \frac{2}{\pi} e^{-2|\beta - \alpha|^2} \end{aligned}$$

Representation of density matrix (4)

Wigner distribution function:

Example (2) :squeezed vacuum state

$$W(y_1, y_2) = \frac{2}{\pi} \exp[-2(y_1^2 e^{-2r} + y_2^2 e^{2r})]$$

Example (3) :fock state $|n\rangle$

$$W(x_1, x_2) = \frac{2}{\pi} (-1)^n L_n(4r^2) e^{-2r}$$

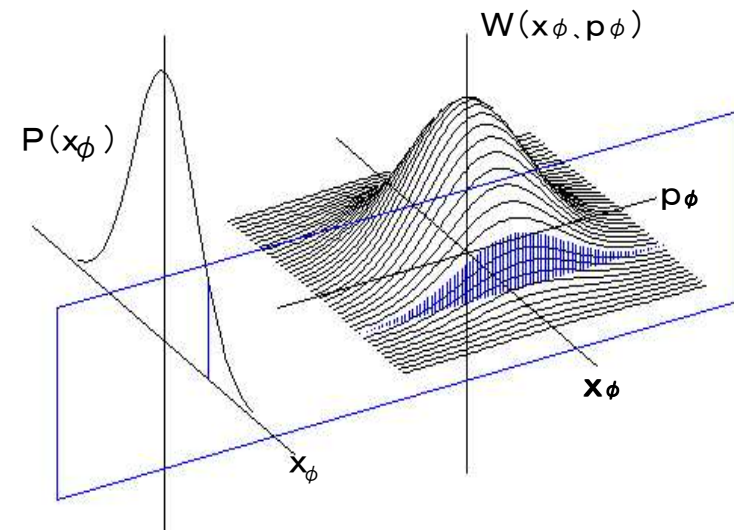
L_n :Laguerre polynomial
can be negative

Relation to homodyne measurement

$$\text{pr}(q, \theta) = \langle q | \hat{U}(\theta) \hat{\rho} \hat{U}^\dagger(\theta) | q \rangle$$

$$\hat{U}(\theta) = e^{-i\theta \hat{a}}, \quad \hat{U}^\dagger \hat{a} \hat{U} = \hat{a} e^{-i\theta}$$

$$\text{pr}(q, \theta) = \int_{-\infty}^{\infty} W(q \cos \theta - p \sin \theta, q \sin \theta - p \cos \theta) dp$$



It is possible to reconstruct Wigner function from homodyne data.

Representation of density matrix (5)

Husimi Q distribution:

$$\chi_A(\eta) = \text{Tr} \left(\hat{\rho} e^{-\eta^* \hat{a}} e^{\eta \hat{a}^\dagger} \right)$$

$$Q(\alpha) = \frac{1}{\pi^2} \int d^2\eta \chi_A(\eta) e^{\eta^* \alpha - \eta \alpha^*}$$

$$Q(\alpha) = \frac{1}{\pi} \langle \alpha | \hat{\rho} | \alpha \rangle$$

$$= \frac{1}{\pi} \int d^2\beta P(\beta) e^{-|\beta - \alpha|^2}$$

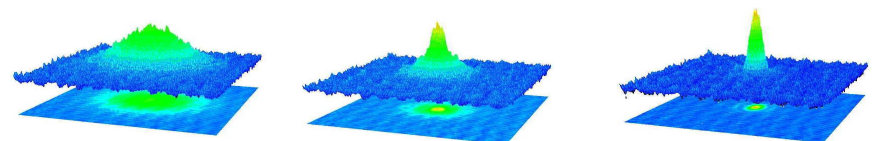
$$\langle \hat{a}^n \hat{a}^{\dagger m} \rangle = \int d^2\alpha Q(\alpha) \alpha^n \alpha^{*m}$$

Outline of the talk

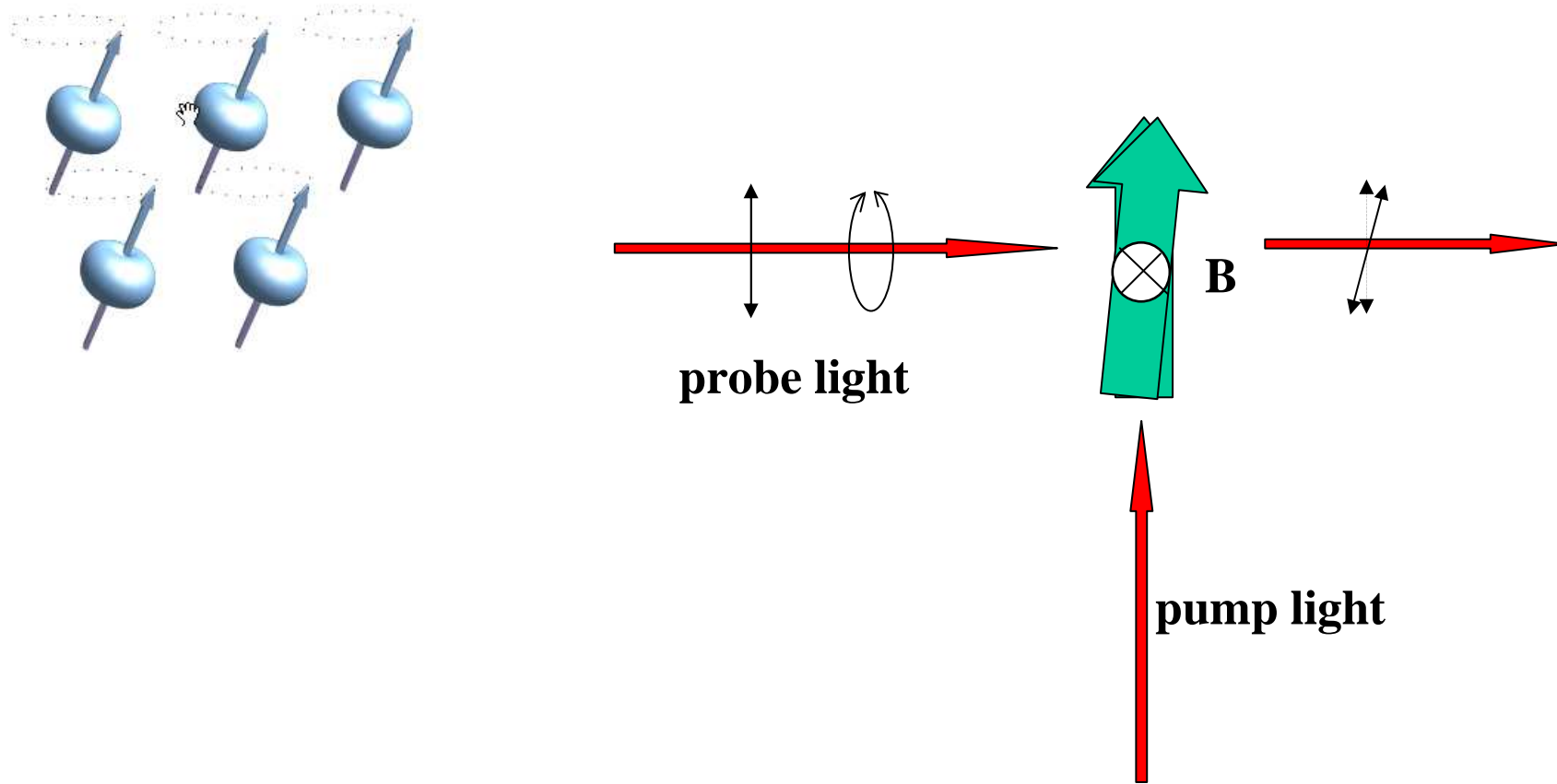
- Introduction
- Quantization of the electromagnetic fields
- Quantum theory of light

Number states (single photon sources),
Coherent states,
Squeezed states,
Homodyne detection

- Nonlinear optics and Quantum state control
- Correlation function
- Representation of density matrix
- Precision measurements using atoms



Atomic Magnetometer



review article: D. Budker and M. Romalis, Nature Phys. 3, 227 (2007).
63

"A subfemtotesla multichannel atomic magnetometer,"

I. K. Kominis, T. W. Kornack, J. C. Allred & M. V. Romalis, Nature, Vol. 422, pp. 596-599 (2003).

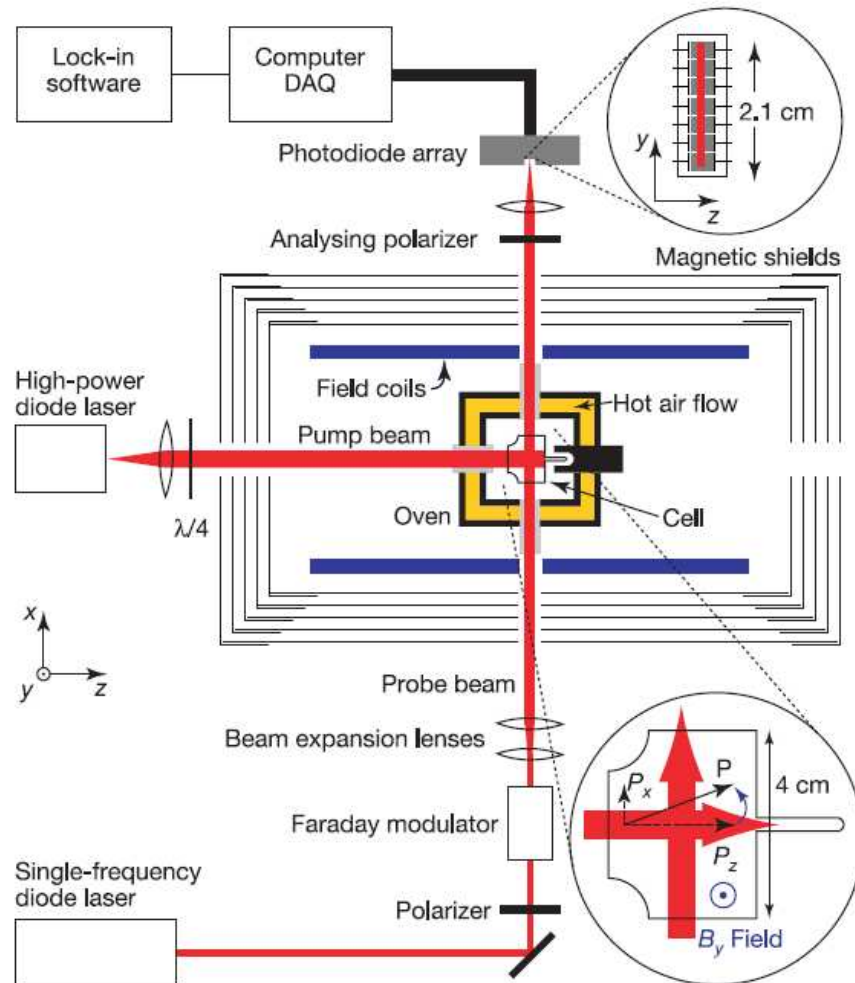


Figure 2 Experimental set-up. The diagram shows: magnetic shields with a shielding factor of 10^6 ; field coils producing calibrated, uniform fields along \hat{x} , \hat{y} and \hat{z} directions, and all five independent first-order field gradients; a T-shaped glass cell ($3 \times 4 \times 3$ cm) with flat windows, containing a drop of K metal, 2.9 atm of ${}^4\text{He}$ and 60 torr of N_2 ; a double-wall oven heated to 180 °C by flowing hot air to obtain a K atom number density of $n \approx 6 \times 10^{13} \text{ cm}^{-3}$; a circularly polarized 1 W broadband diode laser ('pump' laser) tuned to the centre of the D1 line at 770 nm; a linearly polarized 100 mW single frequency laser ('probe' laser) detuned by 1 nm from the D1 resonance; a Faraday rotator modulating the plane of polarization of the probe laser with an amplitude $\alpha \approx 0.02 \text{ rad}$ at a frequency $f_{\text{mod}} = 2.9 \text{ kHz}$; beam-shaping optics that produce a collimated probe beam with a cross-section of 4 mm \times 19 mm; a polarization analyser, orthogonal to the polarizer; a seven-element photodiode array (shown in the top inset), with element separation of 0.31 cm along the \hat{y} -direction; and a 16-bit data acquisition system using a digital seven-channel lock-in amplifier to demodulate the signal proportional to the magnetic field B_y . Bottom inset, cross-section of the T-shaped cell, showing the rotation of the K polarization \mathbf{P} into the \hat{x} direction by an applied magnetic field B_y .

$$\delta B = \frac{1}{\gamma \sqrt{n T_2 V t}} \quad \gamma = g \mu_B / \hbar (2I + 1)$$

"A subfemtotesla multichannel atomic magnetometer,"

I. K. Kominis, T. W. Kornack, J. C. Allred & M. V. Romalis, Nature, Vol. 422, pp. 596-599 (2003).

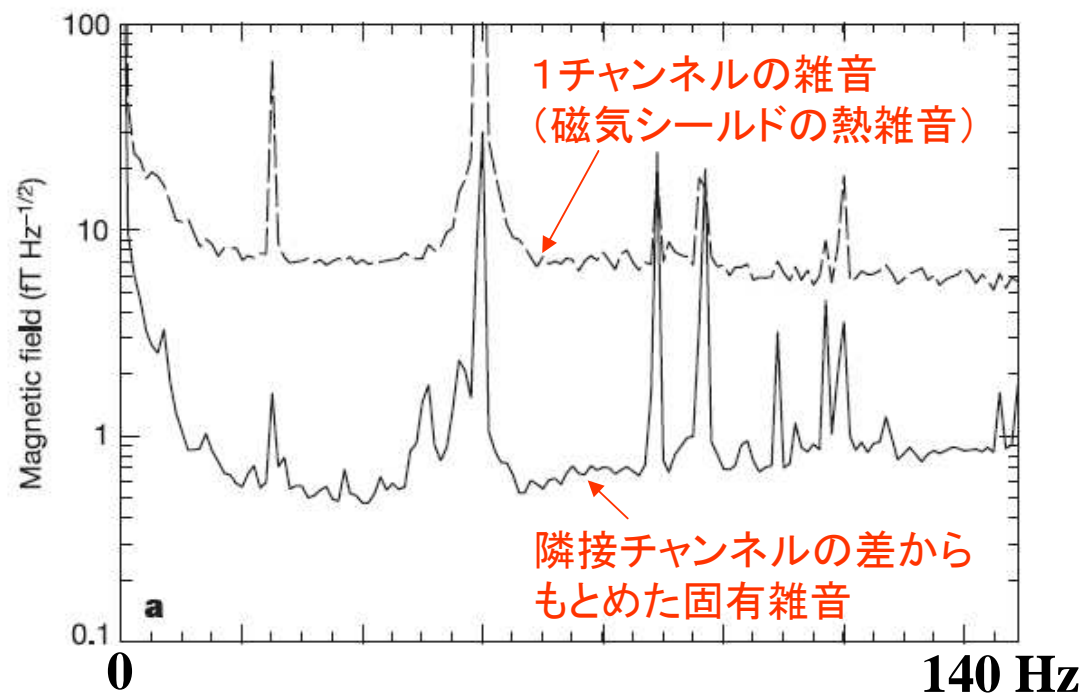
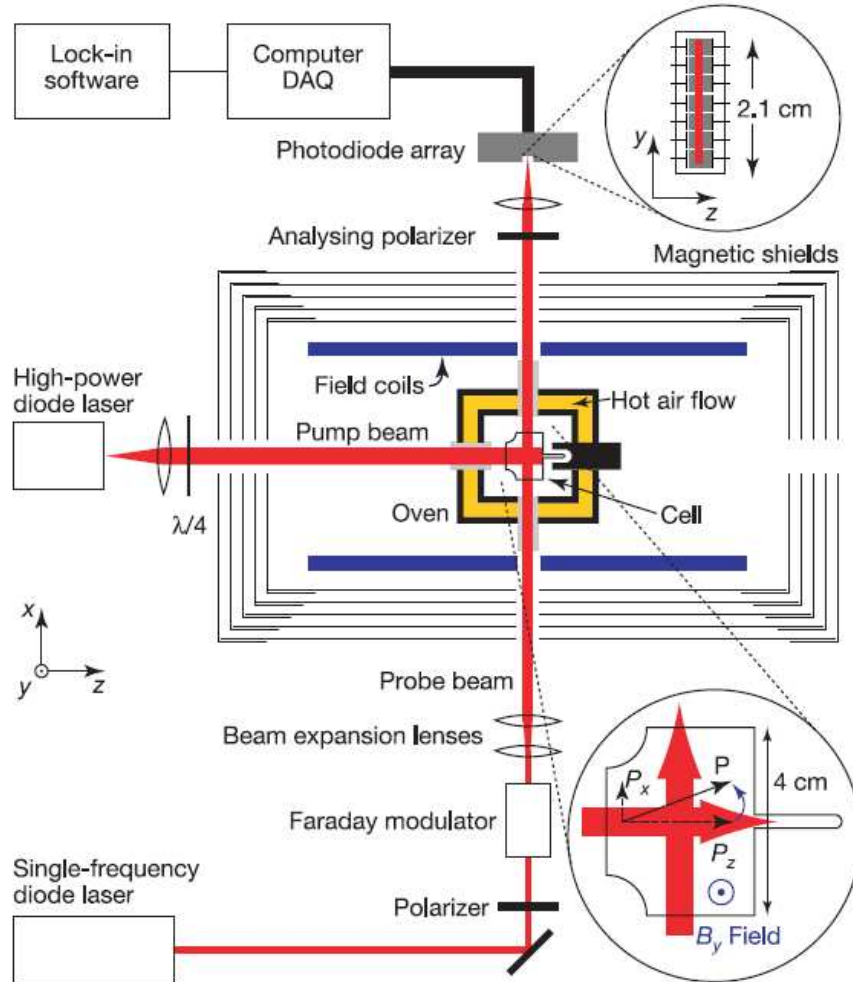
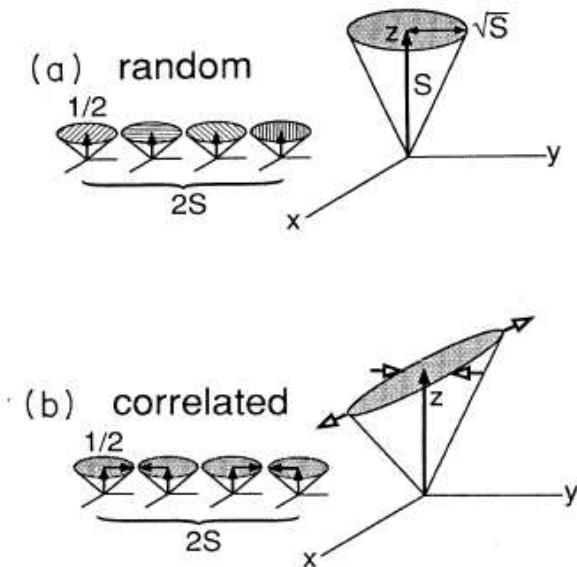


Figure 3 Magnetic field sensitivity and bandwidth of the magnetometer. Magnetic field noise in a single channel (a, dashed line), and intrinsic magnetic field sensitivity of a single channel extracted from the difference between adjacent channels (a, solid line). The magnetic field sensitivity data are obtained by recording the response of the magnetometer for about 100 s, performing a fast Fourier transform (FFT) without windowing; and calculating r.m.s. amplitudes in 1 Hz bins. A peak due to the calibrating B_y field is seen at 25 Hz. To obtain absolute field sensitivity, we divide the magnetometer FFT by a normalized frequency-response function shown in b with a fit to $A/(f^2 + B^2)^{1/2}$,

Quantum magnetometer



“Squeezed spin states,” Masahiro Kitagawa and Masahito Ueda, Phys. Rev. A 47, 5138–5143 (1993)

Angular momentum system

$$\vec{S} = (S_x, S_y, S_z)$$

Cyclic commutation relation

$$[S_i, S_j] = i\epsilon_{ijk} S_k$$

$$\rightarrow (\Delta S_i^2)(\Delta S_j^2) \geq \frac{1}{4} |\langle S_k \rangle|^2$$

For N atoms in $m_F=F$ along the quantization axis z,

$$S_z = FN$$

A magnetic field along y axis causes a rotation of S in x-z plane. Polarization of light propagating along x will be rotated proportional to S_x . This measurement is limited by the projection noise of the atom,

$$(\Delta S_x^2) = \frac{S_z}{2} = FN/2$$

and light shot noise of polarization measurement.

"Sub-Projection-Noise Sensitivity in Broadband Atomic Magnetometry,"

M. Koschorreck, M. Napolitano, B. Dubost, and M. W. Mitchell, Phys. Rev. Lett., Vol. 104, 093602 (2010).

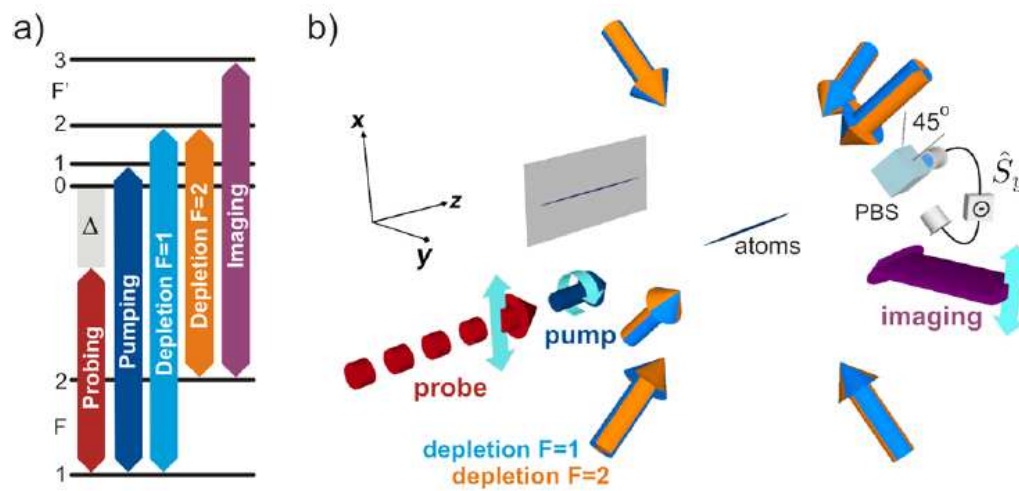


FIG. 1 (color online). (a) Atomic transitions for probing, preparation, and imaging light fields. (b) Atomic ensemble with probing, pumping, and imaging light fields. The polarimeter measures in the 45° basis, i.e., the Stokes component \hat{S}_y .

Laser cooled Rb atoms, 10^6 , $25\mu\text{K}$, dipole trap
20 times QND measurement w/o dipole trap

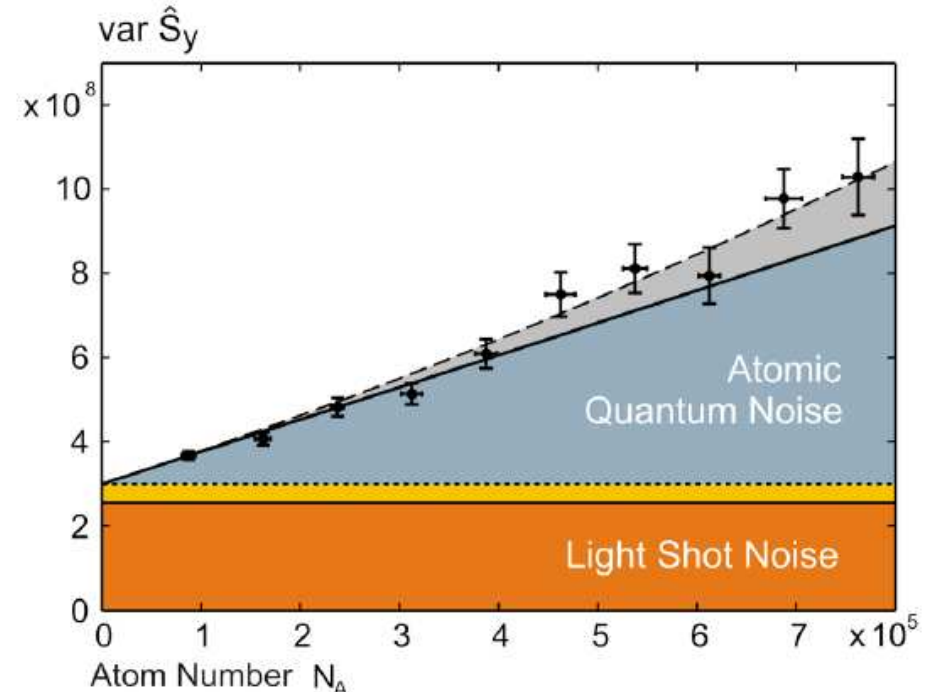


FIG. 3 (color online). Measured variance of \hat{S}_y with statistical errors for $N_L = 10^9$ as a function of atom number. Dashed curve: theoretical curve including technical noise sources. Solid line: pure spin quantum noise. Dotted line: shot noise and technical light noise. Thin solid line: light shot noise. The electronic noise is not plotted because it is negligible for this number of photons.

“Spin Squeezing of a Cold Atomic Ensemble with the Nuclear Spin of One-Half”,
T. Takano, M. Fuyama, R. Namiki, and Y. Takahashi, Phys. Rev. Lett. 102, 033601 (2009).

"Squeezed-Light Optical Magnetometry," Florian Wolfgramm, Alessandro Cerè, Federica A. Beduini, Ana Predojević, Marco Koschorreck, and Morgan W. Mitchell , Phys. Rev. Lett., Vol. 105, 053601 (2010).

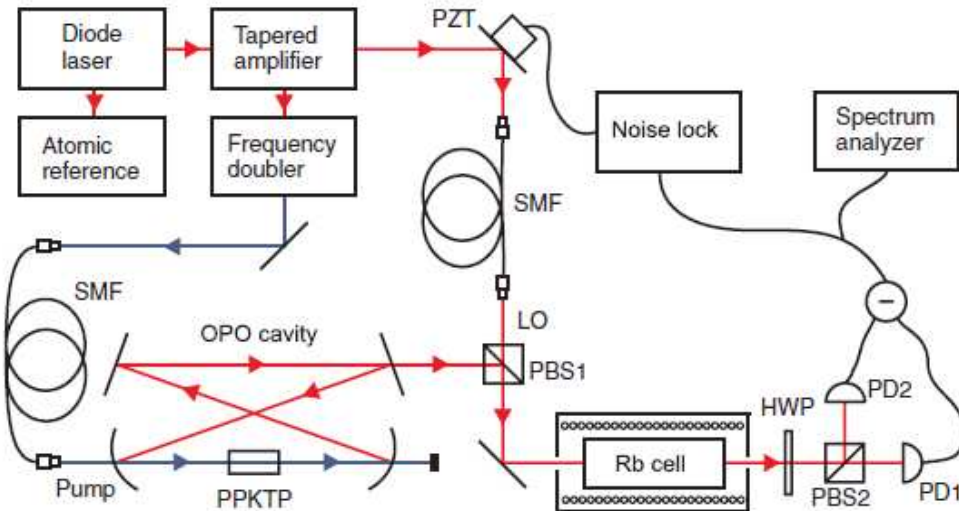


FIG. 1 (color online). Experimental apparatus. Rb cell, rubidium vapor cell with magnetic coil and magnetic shielding; OPO, optical parametric oscillator; PPKTP, phase-matched nonlinear crystal; LO, local oscillator beam; PBS, polarizing beam splitter; HWP, half-wave plate; SMF, single-mode fiber; PD, photodiode.

Hot Rb atoms, 794.7 nm, D1 line

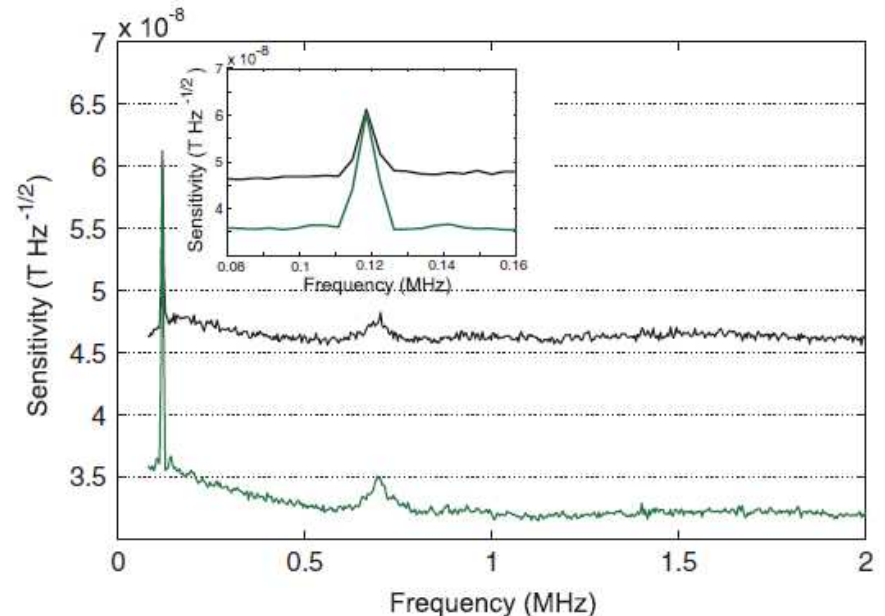


FIG. 3 (color online). Faraday rotation measurement. Power of the polarization signal as center frequency is scanned, $RBW = 3$ kHz, $VBW = 30$ Hz. The (upper) black curve shows the applied magnetic signal at 120 kHz above the shot-noise background of a polarized (but not squeezed) probe. The (lower) green line depicts the same signal with polarization-squeezing. A zoomed view around the calibration peak at 120 kHz is shown in the inset.

-3.2 dB, 3.2×10^{-8} T/ $\sqrt{\text{Hz}}$

Outline of the talk

- Introduction
- Quantization of the electromagnetic fields
- Quantum theory of light
 - Number states (single photon sources),
 - Coherent states,
 - Squeezed states,
 - Homodyne detection
- Nonlinear optics and Quantum state control
- Correlation function
- Representation of density matrix
- Precision measurements using atoms
- Continuous-variable quantum key distribution

A brief review of CV QKD

- Home-(or hetero-)dyne detection is utilized to detect weak light.
→ Quadrature-phase amplitudes (continuous variables) are measured.
 - ◆ merit: room temperature operation with conventional devices
 - ◆ drawback: needs local oscillator phase-locked to the signal
- Quantum states sent by Alice
 - coherent states (easy to generate), or squeezed states, or non-Gaussian
- Coherent-states modulation schemes
 - ◆ Continuous modulation : e.g. Gaussian modulation
Gaussian distribution of quadrature-phase amplitudes
 - ◆ Discrete modulation (i.e. QPSK)
Similarities with QAM optical transmission scheme
Unconditional security proofs have been presented.
- Mode of electromagnetic field
pulsed light, frequency sidebands

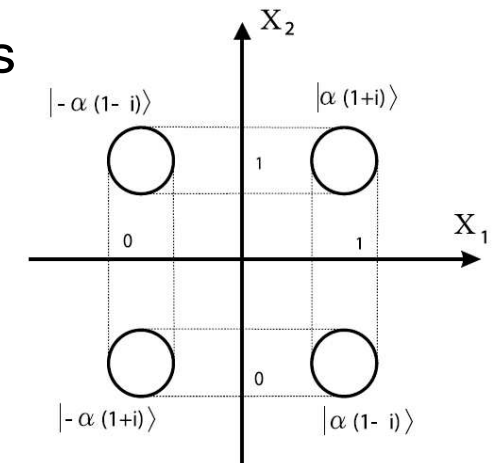


FIG. 5. Phase-space picture of the efficient four-state protocol.

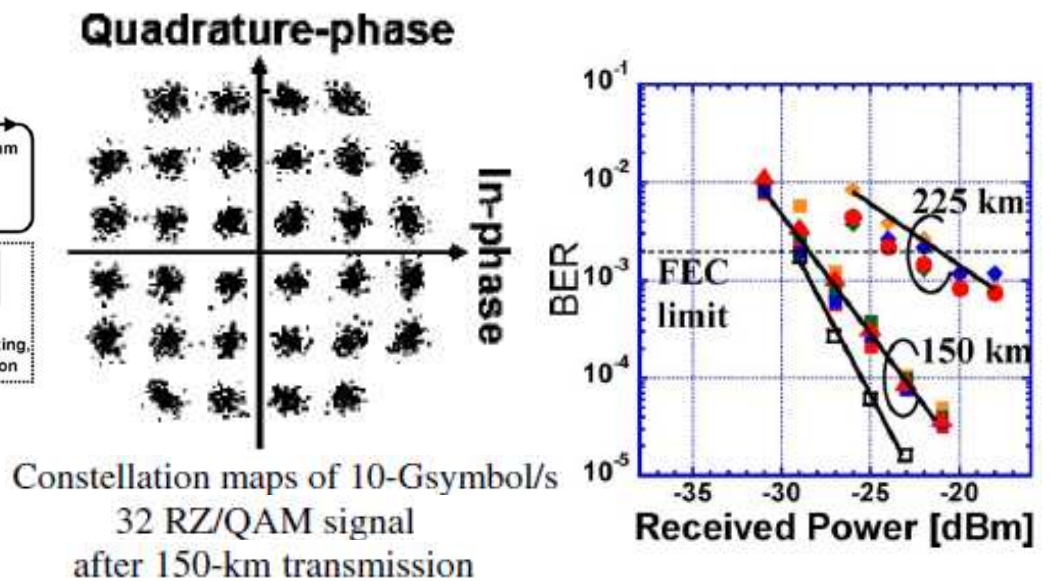
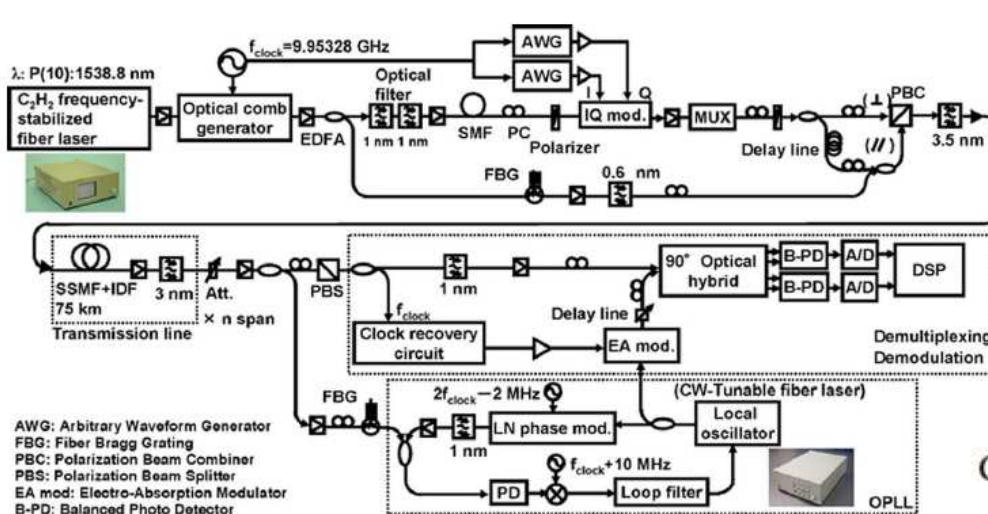
QAM system by Prof. Nakazawa group, Tohoku Univ.

562

IEEE PHOTONICS TECHNOLOGY LETTERS, VOL. 22, NO. 8, APRIL 15, 2010

Single-Channel 400-Gb/s OTDM-32 RZ/QAM Coherent Transmission Over 225 km Using an Optical Phase-Locked Loop Technique

Keisuke Kasai, *Member, IEEE*, Tatsunori Omiya, Pengyu Guan, *Student Member, IEEE*, Masato Yoshida, Toshihiko Hirooka, *Member, IEEE*, and Masataka Nakazawa, *Fellow, IEEE*

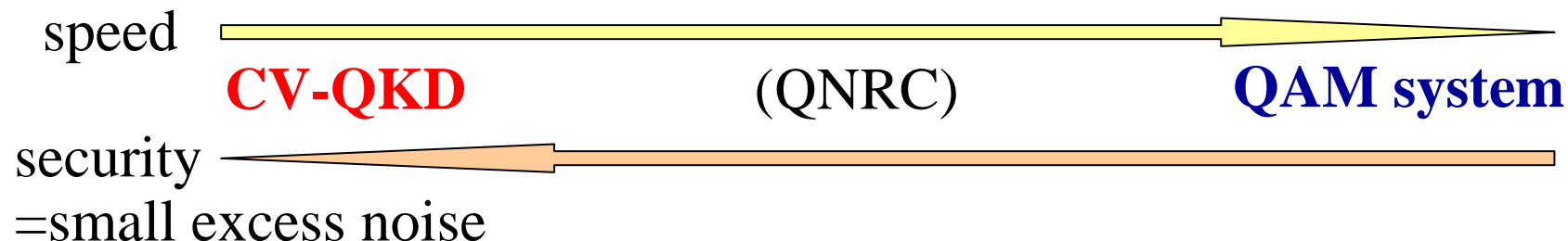


CV QKD and QAM optical transmission

Similarities

- ◆ Coherent states modulated in phase-space are sent
 - ◆ Homodyne detection is utilized to readout quadrature-phase amplitudes
- ➡ A coherent optical communication system operating in quantum noise limit is ready for CV QKD.

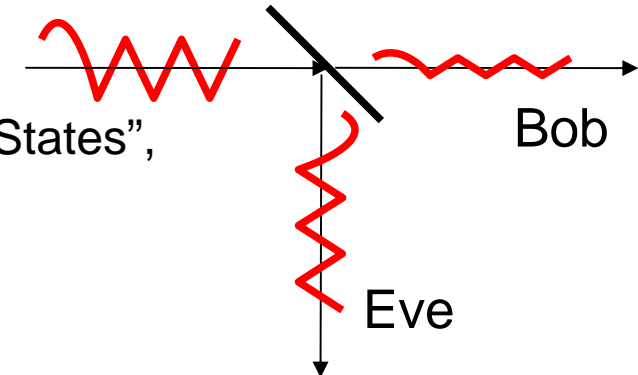
Similarities between the QAM optical communication and the CV-QKD may allow us in future to perform both high speed data transmission and unconditionally secure QKD with same equipments by switching its operation mode.



CV QKD and 3-dB loss limit

3dB loss limit

"Continuous Variable Quantum Cryptography Using Coherent States",
F. Grosshans and P. Grangier, PRL **88**, 057902 (2002).



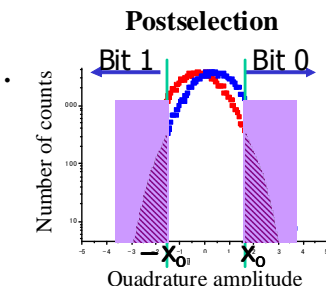
Recipe for beating 3dB-loss-limit

Post-selection

"Continuous Variable Quantum Cryptography: Beating the 3 dB Loss Limit",
Ch. Silberhorn, T. C. Ralph, N. Lütkenhaus, and G. Leuchs, Phys. Rev. Lett. 89, 167901 (2002).

"Quantum cryptography using balanced homodyne detection,"
T. Hirano, T. Konishi, R. Namiki, quant-ph/0008037; Extended abstract for EQIS 2001.

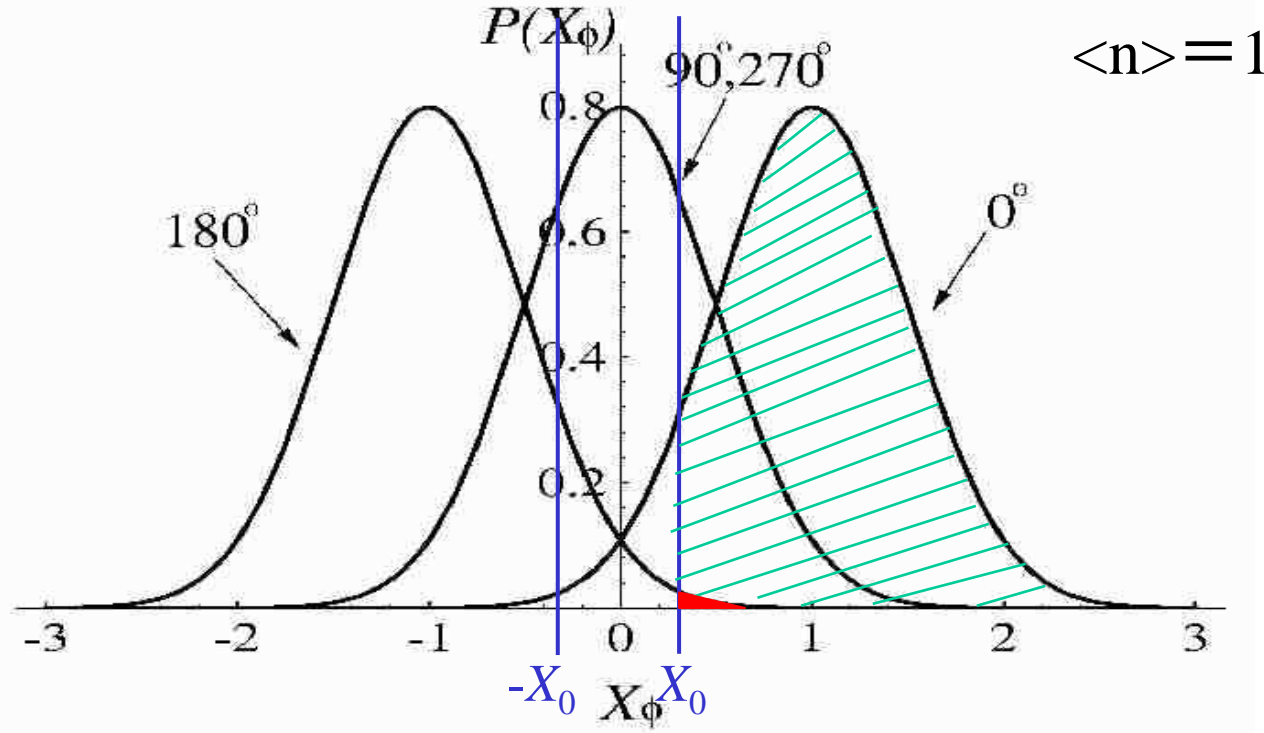
"Security of quantum cryptography using balanced homodyne detection",
R. Namiki, T. Hirano, Phys. Rev. A, vol. 67, no.2, 022308-1-7 (2003).



Reverse reconciliation

"Quantum key distribution using gaussian-modulated coherent states" , F. Grosshans, G. Van Assche, J. Wenger, R. Brouri, N. J. Cerf, Ph. Grangier, Nature **421**, 238 (2003).

Probability distribution of quadrature amplitude



Bob sets up a threshold value X_0 .

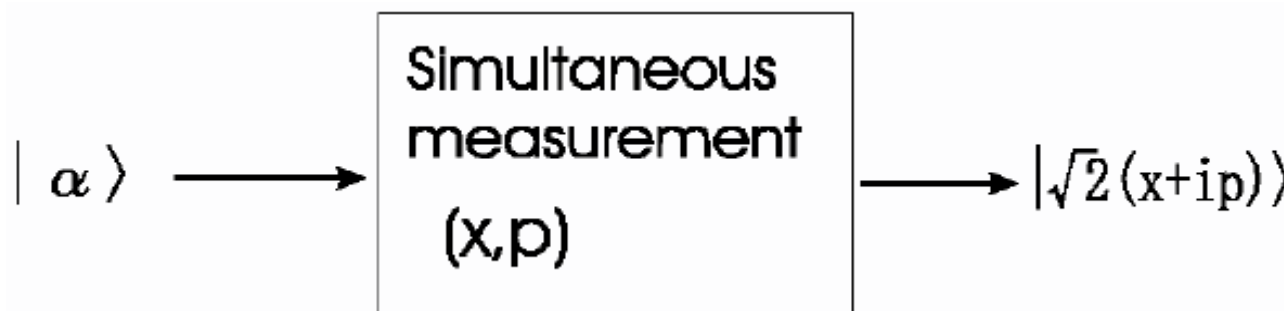
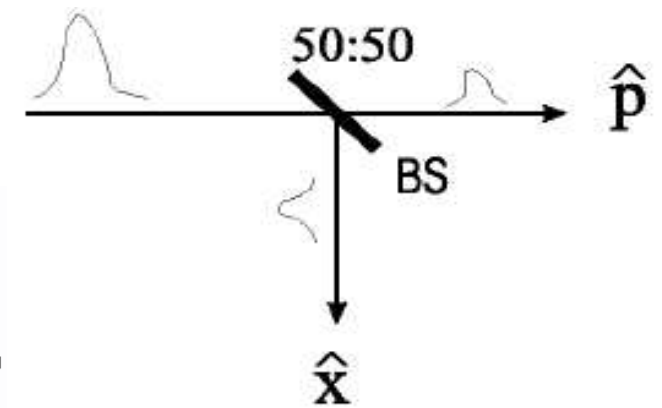
- { If the measured value $X_\phi < -X_0$, Bob judges that $\phi = 180^\circ$.
- { If $X_\phi > X_0$, Bob judges that $\phi = 0^\circ$.
- If $-X_0 < X_\phi < X_0$, Bob abandons the judgement.

Increasing X_0 , the error rate, e_B , decreases to an arbitrary small value.
The “effective” detection efficiency, P , also decreases.

Security of CV QKD: loss limit caused by excess noise (1)

R. Namiki and TH, Phys. Rev. Lett., vol. 92, 117901 (2004).

1. Eve performs a simultaneous measurement on both quadrature amplitudes (x, p) using a beam splitter.
2. Eve resends a coherent state $|\sqrt{2}(x+ip)\rangle$ to Bob.

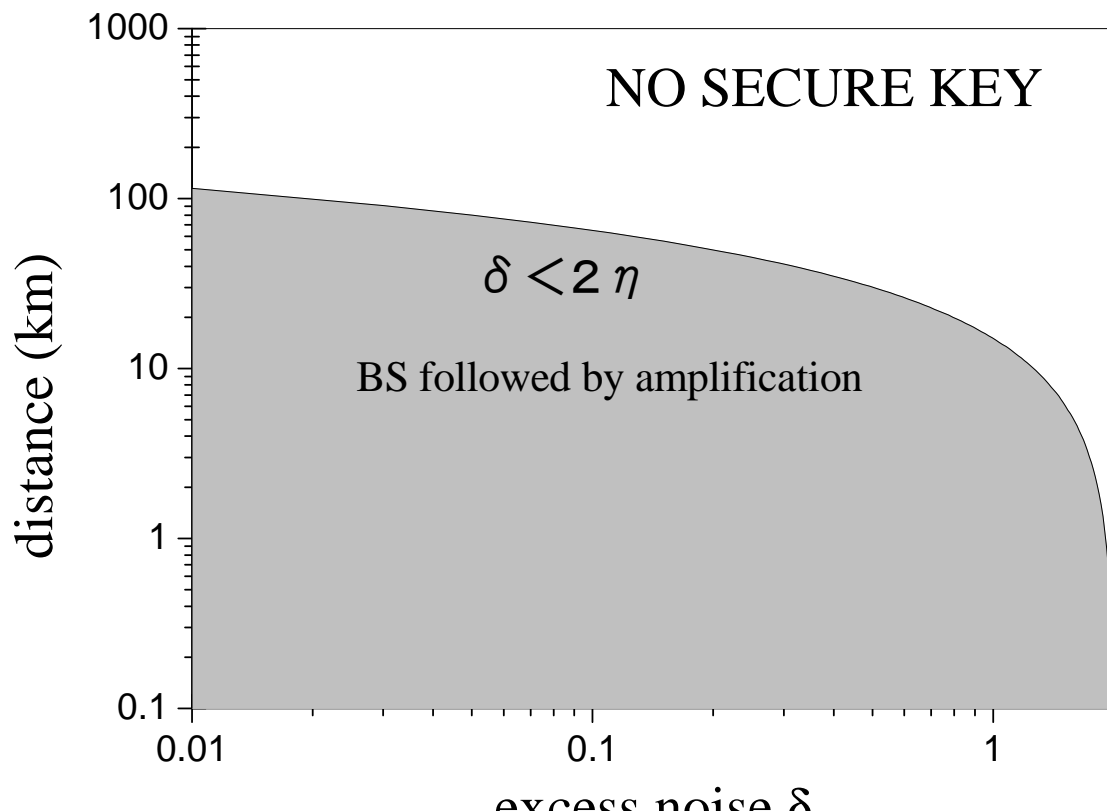


No secret key because Eve knows the state that Bob measures.
(entanglement breaking)

Applicable to any CV QKD protocol using coherent states and homodyne detection

Security of CV QKD: loss limit caused by excess noise (2)

R. Namiki and TH, Phys. Rev. Lett., vol. 92, 117901 (2004).



Define excess noise δ :

$$\delta = \frac{(\Delta x_{\text{obs}})^2}{(\Delta x)^2} - 1$$

Intercept & resend attack increases excess noise:

$$\delta = 2.$$

Excess noise decreases by loss:

$$\delta = 2\eta, \quad \eta: \text{transmissivity}.$$

$\delta < 2\eta$ is a necessary condition.

Excess noise should be small for unconditional security.

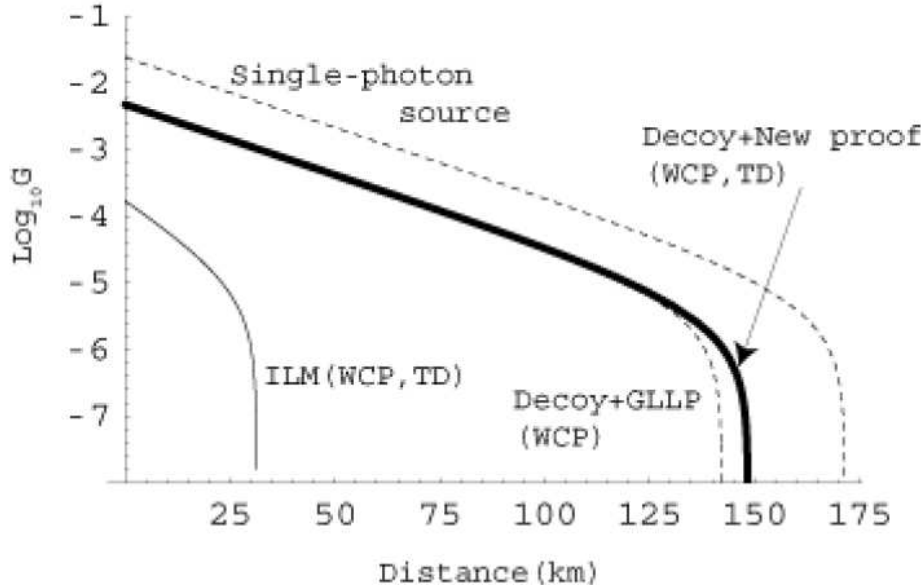


FIG. 3: The net key generation rate G (bits per pulse) vs distance. WCP and TD means that the curve is valid when weak coherent-state pulses and threshold detectors are used, respectively. Parameters used are from [18]: $d = 1.7 \times 10^6$, $\eta_d = 0.045$, $f(E) = 1.22$, the fiber loss 0.21 db/km, and 3.3% of distance-independent contribution to the QBER.

M. Koashi, quant-ph/0609180

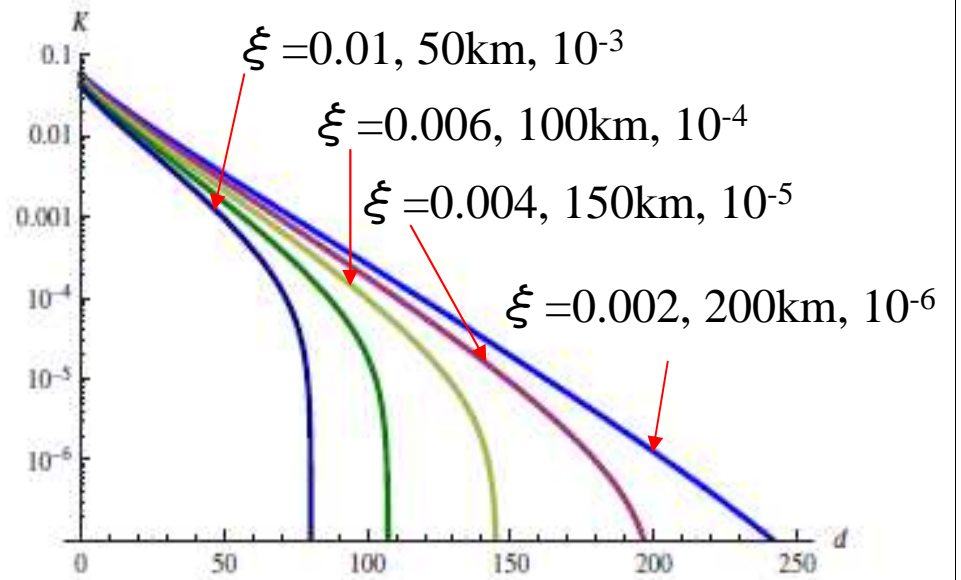


FIG. 2 (color online). Secret key rate as a function of the distance for different values of the excess noise: from top to bottom, $\xi = 0.002, 0.004, 0.006, 0.008, 0.01$. The quantum efficiency of Bob's detection is $\eta = 0.6$. 0.2 dB/km

Anthony Leverrier and Philippe Grangier,
Phys. Rev. Lett., 102, 180504 (2009).
(Erratum: PRL 106, 259902 (2011).)

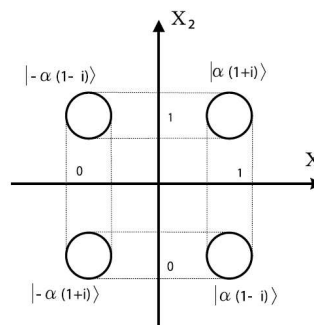


FIG. 5. Phase-space picture of the efficient four-state protocol.